Browse all Theses and Dissertations

Theses and Dissertations

2013

# The Enhancement of Peroxide-Cured Fluoroelastomer Rubber to Metal Bonding

Richard Hunter Cooke III
*Wright State University*

THE ENHANCEMENT OF PEROXIDE-CURED FLUOROELASTOMER RUBBER TO
METAL BONDING


A thesis submitted in partial fulfillment
of the requirements for the degree of
Master of Science


By


Richard Hunter Cooke III
B.S., Northern Kentucky University, 2011


2013
Wright State University

WRIGHT STATE UNIVERSITY

GRADUATE SCHOOL

June 4, 2013

  I HEREBY RECOMMEND THAT THE THESIS PREPARED UNDER MY SUPERVISION BY  Richard Hunter Cooke III  ENTITLED The Enhancement of Peroxide-Cured Fluoroelastomer Rubber to Metal Bonding BE ACCEPTED IN PARTIAL FULFILLMENT OF THE REQUIREMENTS FOR THE DEGREE OF Master of Science .

               _____

               Eric Fossum, Ph.D., Director
               Department of Chemistry
              College of Science and Mathematics

               _____

               David A. Grossie, Ph.D., Chair
               Department of Chemistry
              College of Science and Mathematics

Committee on Final Examination

_____
   Eric Fossum, Ph.D.

_____
   David A. Dolson, Ph.D.

_____
   Kenneth Turnbull, Ph.D.

_____
   Steve Glancy, Ph.D.

_____
   R. William Ayres, Ph.D.
  Interim Dean, Graduate School

# ABSTRACT

Cooke III, R. Hunter. M.S., Department of Chemistry, Wright State University, 2013. The Enhancement of Peroxide-Cured Fluoroelastomer Rubber To Metal Bonding.

A "combi-cured" fluoroelastomer (FKM) rubber formulation was designed to yield 100% cohesive rubber failure when cured to cold-rolled steel with derivatives of polymeric silane adhesives.  Three different categories of adhesives were tested: Unsaturated Polymeric Silane with Phosphonium Salt (UPSP-D), Unsaturated Polymeric Silane (UPS-L), and Saturated Polymeric Silane (SPS-L).  Adhesion Inserts molded using ASTM Method D429 Method C all consistently yielded 100% cohesive rubber failure and showed adhesion strength in the range of 700 to 800 psi after being pulled at 2" per minute until break.  After obtaining consistent 100% rubber failure, a design of experiment (DOE) was implemented to determine optimum metal pretreatment conditions as well as optimal rubber ingredients to yield maximum rubber retention and adhesion strength.  A method was also developed to determine the locus of failure when the failure occurred at an interface using Attenuated Total Reflectance Fourier Transform Infrared Spectroscopy (ATR FT-IR).

**TABLE OF CONTENTS**

**TABLE OF CONTENTS (continued)**

# LIST OF TABLES

# LIST OF SCHEMES

# LIST OF EQUATIONS

**DEDICATION**

It is my honor to dedicate this thesis to my parents, Rick and Bonnetta Cooke, my sister, Ashley Cooke, and my aunt, Shirley Willis.  Their love and continued support has brought me to and through this important milestone in my education.  I love all of you and cannot thank you enough.   I would also like to dedicate this to Matthew Tyler and Isaac Valentino Willis who have been a great source of joy over the past few years.  I cannot wait to see the young men you grow up to be!

## ACKNOWLEDGEMENTS

I would like to first thank Dr. Eric Fossum for allowing me to join his research group. I am grateful for constant support, patience, and teaching over the last two years. I would also like to thank Drs. Steve Glancy and Mahmoud Kardan as well as Bob Ferguson for their constant support as well as mentorship with this project.

I would like to thank Vernay Laboratories for funding this project as well as all of the employees at the Yellow Springs, OH facility for accepting me in the community and allowing me to be a valued member of the team during my time with Vernay.

I would also like to thank the faculty and staff in the Chemistry Department at Wright State University for the valued education I have been lucky to receive over my time at WSU.

Lastly, I would like to thank my fellow graduate students, specifically Dr. Fossum's group, for all of the memories I will be sure to carry with me for many years.

# 1.    Introduction

Globally, adhesives are used in a variety of ways and in 2009 were estimated to have a size of roughly 16.6 billion pounds, which made the adhesive industry have a market value of an estimated \$20.6 billion. [1] The use of fluoroelastomers has been rapidly expanding since their birth in the 1950's. [2,3] The superior physical and chemical properties of fluoroelastomers have led to the need for the current kind of study, which involves optimizing the adhesion of peroxide cured fluoroelastomers to cold-rolled steel.

## 1.1    Fluoroelastomers

Fluoroelastomers (FKMs) are fluorine containing, cross-linked, semi-crystalline or amorphous polymers that have a carbon-carbon moiety for their backbone, **Figure 1**. [2] FKMs are distinguished from closely related perfluoroelastomers by the presence of the methylene group ($-CH_2-$) in the backbone of the polymer.

$$\sim\overset{\displaystyle F}{\underset{\displaystyle F}{C}}-\overset{\displaystyle H}{\underset{\displaystyle H}{C}}-\overset{\displaystyle F}{\underset{\displaystyle F}{C}}-\overset{\displaystyle CF_3}{\underset{\displaystyle F}{C}}\sim$$
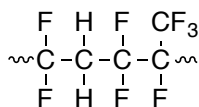
**Figure 1**: Generic example of FKM

The amorphous nature of the polymer allows the polymer to maintain elastomeric properties, meaning that the polymer is flexible and recovers from reasonable amounts of stress at temperatures above $0^{\circ}C$. [4] FKMs are known to be

very versatile and have the ability to be either semi-crystalline or completely amorphous.[5] This versatility along with superior properties in regards to chemical and oxidative resistance as well as weathering resistance,[2,6] allow FKMs to be great materials for many industries including: automotive, aerospace, chemical engineering, and microelectronics where they are used in applications such as graffiti-resistant paint and high-performance O-rings.[2,5,6] **Figure 2** is a representation showing the swell and heat resistance of many commercially available elastomers. The figure illustrates the superiority of FKM in regards to heat and oil resistance.
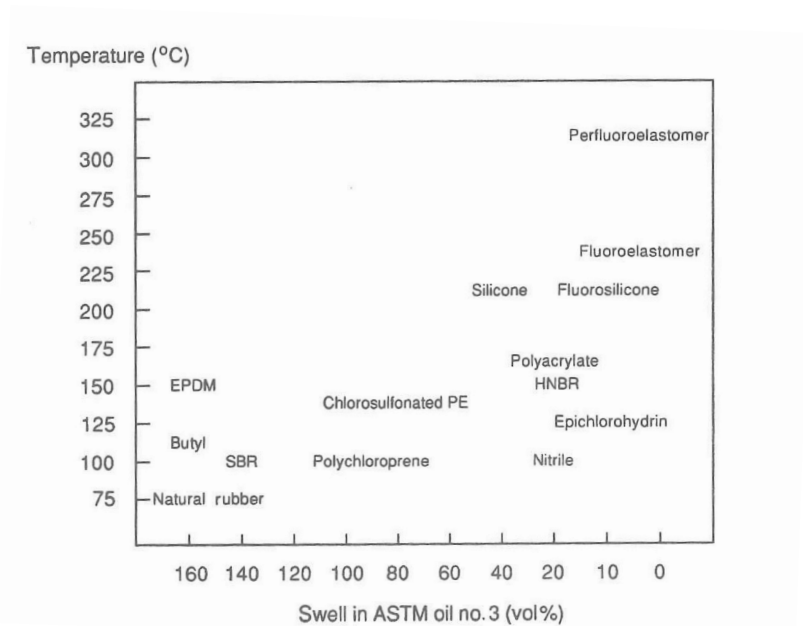


**Figure 2:** Heat and chemical resistance of FKMs. This image is a reprint of Figure 32.2 from Modern Fluoropolymers with permission from John Wiley and Sons.

The superior chemical properties can be attributed to the high electronegativity of the fluorine atom (3.98)[7] as well as the nature of the C-F and C-C bonds, which comprise the majority of the compound.[4-6,8,9] The C-F bond has one of the highest bond energies in organic chemistry (480 kJ/mol).[10] The low

polarizability of the bond ($0.56 \times 10^{-24}$) [10] causes very weak London dispersion forces, which is believed to afford the extreme hydro- and lipophobicity of the bulk material.[8,10]

### 1.1.1 Early Fluoropolymers

The first fluoropolymers, low-molecular weight poly(cholorotrifluoroethylene)s, were synthesized in the late 1930s, followed by the accidental discovery of high-molecular weight poly(tetrafluoroethylene) (PTFE) (Teflon ®).[6,11] The chance discovery of PTFE was found at the hands of Roy Plunkett who compressed tetrafluoroethylene (TFE) but later found that there was no pressure and that the compound spontaneously polymerized. [7,12] Since then, a more controlled method for polymerization has been developed and currently there are multiple procedures commonly employed. The general method is to polymerize TFE as seen in **Scheme 1** but the specifics of the polymerization can be tailored to suit the desired end product. [7,12,13]

**Scheme 1**: The polymerization of PTFE from TFE.
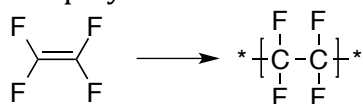


PTFE is extremely well known for its many favorable properties including: hydrophobicity, chemical inertness, low coefficient of friction and crystallinity. [13,14] These properties make it a suitable candidate for such diverse applications as: cookware, nail polish, and windshield wiper blades. [15]

The accidental discovery of PTFE led to the purposeful syntheses of many polymeric fluorine-containing materials, such as poly(vinlyidene fluoride) (PVDF).

**Scheme 2**: Polymerization of PVDF from VDF.
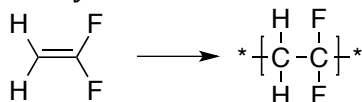


The most common method to make PVDF is by free-radical polymerization of vinylidene fluoride (1,1-difluoroethylene) (VDF) (**Scheme 2**). Typically, an organic or inorganic peroxide is utilized as the initiator and the reaction is carried out in water, via either an emulsion or suspension process. In both processes a large range of heat ($10°C$ to $130°C$) and pressure (10 atm to 200 atm) are required.[16] This yields a high molecular-weight, semi-crystalline thermoplastic polymer that is approximately 50 % crystalline.[9,17-19] PDVF has been well documented for its piezoelectric properties due the nature of its microstructure.[11,17-20] Although the sometimes semi-crystalline nature of PTFE and PVDF alone allows great opportunity for applications in many facets of materials science, it does not afford the materials the unique properties to be a suitable fluoroelastomer.[9,13,16,21]

The US Air Force developed a need to upgrade the material for a series of elastomer-based O-rings in the 1950's. These new materials were to be used primarily at low temperatures, but also needed to be versatile enough that they could seal hot engine fluids and hydraulic lubricants.[2,3] The requirements were for an elastomer having superior oil and thermal resistant properties, for which fluoroelastomers seemed likely candidates. Some of the materials that were eventually developed were copolymers using PVDF.

PVDF copolymers fall into three categories: 1) the amount of PVDF far exceeds that of the comonomer, this results in a thermoplastic with lower crystallinity than that of PVDF. 2) A copolymer with slightly higher amounts of the non-VDF comonomer yields a thermoplastic elastomer, and 3) with an even larger amount of non-VDF comonomer yields amorphous, elastic copolymers with low intermolecular forces.[9] This effect is due to the non-VDF comonomer disrupting crystallinity and allowing the polymer to behave more like an amorphous system.[8]

The latter two categories, along with the introduction of perfluoro-methy vinyl ether (PMVE) in the range of 1-5 mol%, has become a commercial way to make FKMs. These PMVE segments further disrupt order in the polymer and antagonize the crystallinity, but do not adversely affect the physical properties unique to FKMs while increasing the overall fluorine content. [22] In addition to decreasing the crystallinity, PMVE is known to decrease $T_g$ while simultaneously increasing resistance to hydrocarbons and polar solvents.[4]

### 1.1.2 FKM Cure Systems

There are three major cure systems for FKM: 1) Diamine, 2) Bisphenol, and 3) Peroxide. The diamine, the original cure system, was used in the reaction to both create points of unsaturation by dehydrofluorination as well as serving the role of the crosslinker itself. Inorganic bases included in the system were used as acid acceptors. The diamine and bisphenol cure react using a similar general mechanism as shown in **Scheme 3**.

The nucleophile "Nu" seen in **Scheme 3** is either an amino derivative or phenolic.

**Scheme 3:** Crosslink formation by nucleophile. The nucleophile can be either an amino or phenolic derivative.
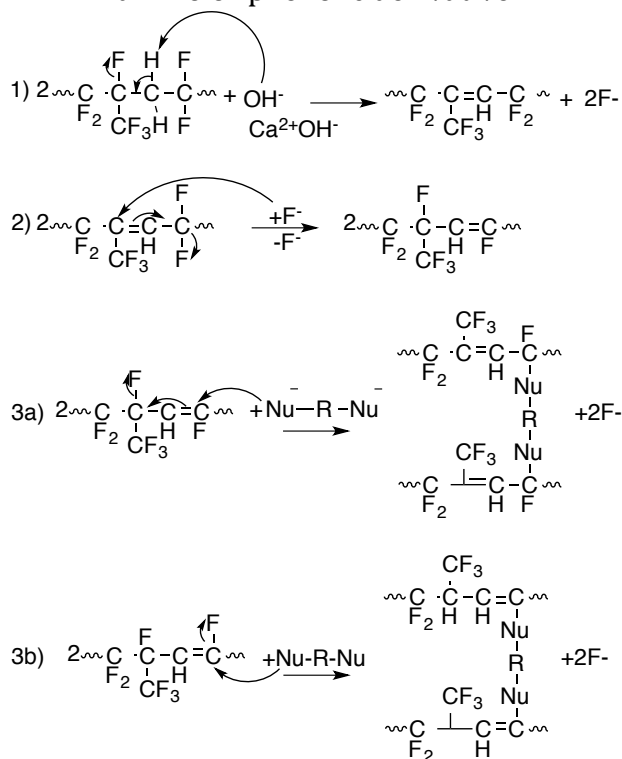


The mechanism generally involves three steps: 1) dehydrofluorination of the polymer with the base (typically calcium hydroxide) to yield unsaturation, 2) rearrangement of the double bond catalyzed by $F^-$ and formation of the more stable $-CH=CF-$, and 3) nucleophilic addition to the product from step 2, which occurs with either a) allylic displacement of fluoride or b) an addition followed by fluoride elimination on the double bond. One of the issues with the diamine cure is that the neutralization of HF by the inorganic bases yielded water, which needed to be removed by a post cure. [4,6]

Multiple issues with the diamine cure eventually led to the development of the bisphenol cure methodology. This system had the ability to achieve much higher levels of cure and it was considered to have increased scorch safety. The bisphenol cure system can use a phosphonium salt as a catalyst, **Figure 3** and was discovered by Schmiegel et. al. [4,6,23,24].
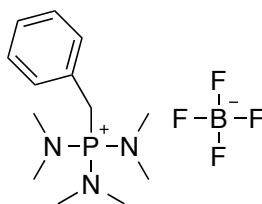


**Figure 3:** An example of a phosphonium salt which catalyzes bisphenol curing. This salt is benzyltris(dimethylaminato)phosphorus[1+] tetrafluoroborate[1-].

The use of the accelerator changes the initial steps of the reaction scheme for the bisphenol system, which can be seen in **Scheme 4**.

**Scheme 4:** The bisphenol cured mechanism with a catalyst.
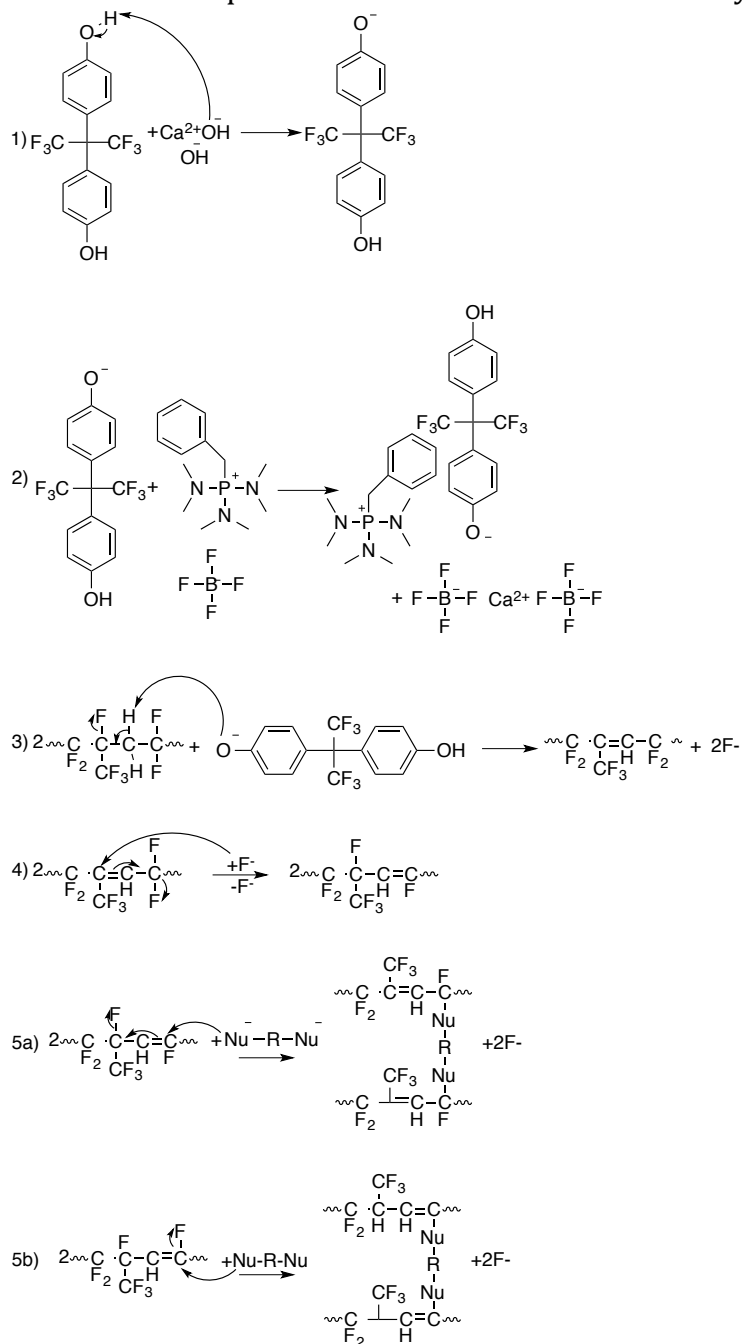


The entire bisphenol mechanism occurs in five steps: 1) The bisphenol reacts with the metal oxide to give a phenolate ion, 2) this ion then reacts with the phosphonium, giving a highly reactive intermediate. 3) The intermediate introduces points of unsaturation in the polymer backbone by dehydrofluorination, 4) the

unsaturation rearranges and the step happens again yielding a diene. 5) A second phenolate attacks the diene leading to dienic phenyl ether crosslinks by either: a) allylic displacement or b) addition followed by fluorine elimination on the double bond. [4,23-25]

The third cure system, peroxide cure, is free radical based.  The peroxide cure offers the benefit of requiring relatively little unsaturation, which renders a final material more resistant to steam and aqueous acid, however, the trade-off is lower thermal stability. [4,25] In order for the peroxide cure system to be effective cure-site monomer (CSM) must be incorporated into the polymer chain.  A CSM typically possesses a relatively labile carbon-bromine or carbone-iodine bond. In addition a crosslinking agent, such as triallyl isocyanurate (TAIC) is necessary (**Figure 4**).  TAIC has three sites susceptible to peroxide cure and the elastomer is able to crosslink through the sites. [3,4,8,9,26]
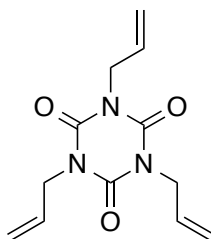


**Figure 4:** The structure of triallyl isocyanurate (TAIC) has three sites susceptible to radical attack.

The mechanism for the peroxide cure, **Scheme 5**, is six steps: 1) Upon exposure to heat the peroxide decomposes generating a radical.  2) The radical then rearranges to give a methyl radical.  3) The methyl radical attacks one point of unsaturation in TAIC generating the TAIC radical.  4) The TAIC radical can then react

with the polymer through the CSM generating a polymer radical.  5) The polymer

radical can react with a second TAIC, which creates a crosslink site between the

polymer and TAIC.   6) This process occurs until a fully crosslinked network is

developed.

**Scheme 5**: Peroxide cured system through TAIC. "X" can be bromine but is likely to be iodine.
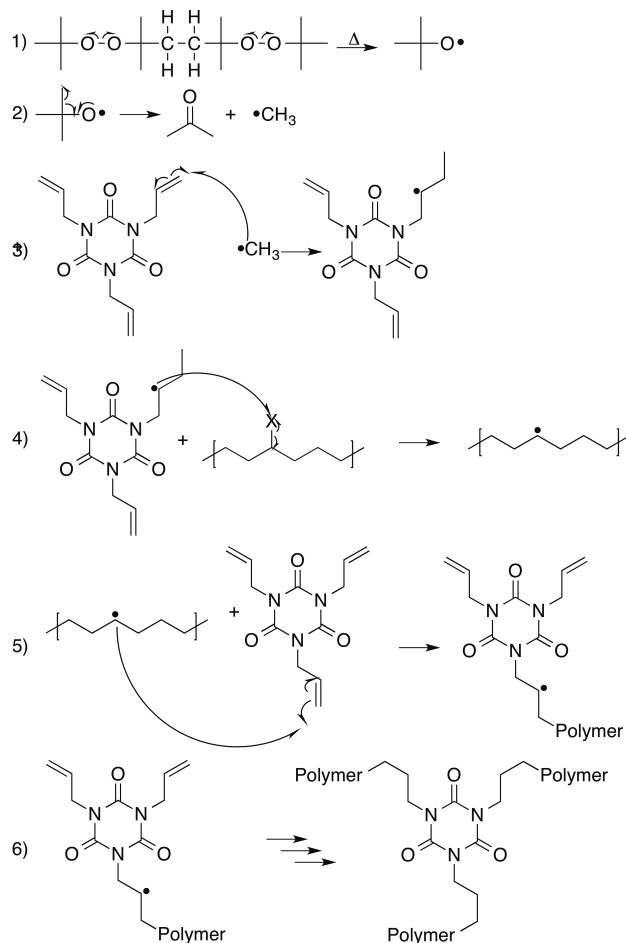
### 1.1.3 Poly[vinylidene fluoride-co-tetrafluoroethylene-co-perfluoro(methyl vinyl ether)-co-iodotrifluoroethylene] (PVTEM)

One of the more common commercially available elastomers is a tetrapolymer, poly[vinylidene fluoride-*co*-tetrafluoroethylene-*co*-perfluoro(methyl vinyl ether)-*co*-iodotrifluoroethylene] (PVTEM), **Figure 5**.
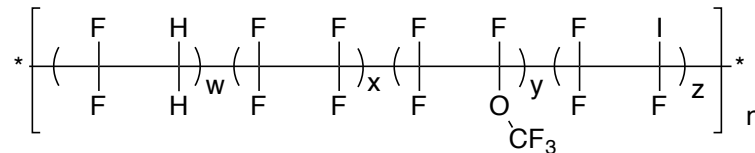


**Figure 5:** Structure of poly[vinylidene fluoride-co-tetrafluoroethylene-co-perfluoro(methyl vinyl ether)]-*co*-iodotrifluoroethylene).

PVTEM takes advantage of the previously mentioned characteristics of the homo- and copolymers. The copolymerization of PVDF and PTFE allows the bulk material to have the thermal and solvent resistivity desired with the extreme applications for FKMs while also sufficiently disrupting the symmetry of the polymer chains, leading to a more amorphous morphology.[27] The addition of PMVE further decreases the $T_g$ and crystallinity, which allows the material to have elastomeric properties at lower temperatures.[6,22,26] The use of the CSM along with certain coagents allows the rubber to cure by radical polymerization giving it superior resistance to aqueous media and allowing for greater scorch safety.[4]

### 1.2 Adhesion

Adhesion is the attraction between two different materials when they are in contact.[28,29] An adhesive, as defined by ASTM D907-06, is "a substance capable of

holding materials together by surface attachment." [28]   The property that allows a single material to attract itself is known as cohesion. [28] The two properties are illustrated in **Figure 6**.
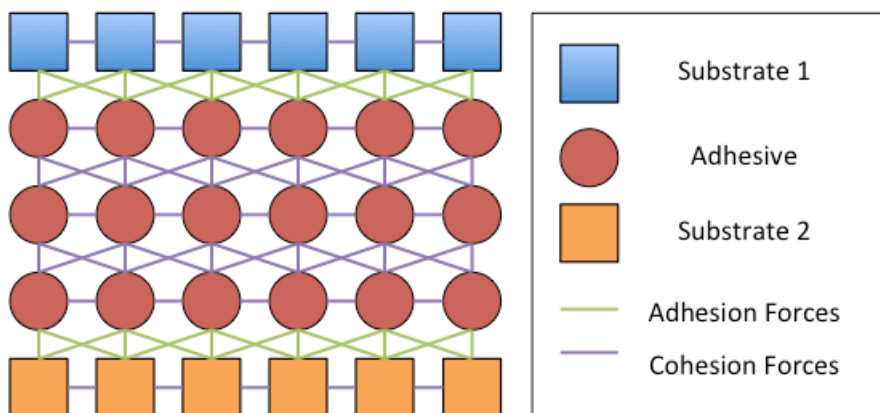


**Figure 6:** Illustration showing adhesion and cohesion forces of generic substrates.

There are three major categories of adhesion: 1) non-bonded interactions, 2) bonding interactions, and 3) mechanical adhesion.  The first is characterized by non-bonding interactions such as: dipole-dipole interactions, hydrogen bonding, and London dispersion forces.   Non-bonding interactions are always present and generally play a minor role relative to the other adhesion interactions.  The second, bonding interaction, is characterized by the introduction of chemical bonds including: ionic, covalent and coordinate bonding.   The final type of bonding, mechanical, is characterized by interlocking the two substrates and is generally the most effective. [30,31]  Since non-bonding interactions occur whenever any of the other categories of adhesion occur, this adhesion type will not be discussed individually, rather concurrently with the other categories.

When studying adhesion there are multiple elements that need to be considered: 1) Type of adhesion, 2) Characterization of the adhesive (or cohesive) interfaces, 3) Destruction of the interfaces via mechanical bond testing, and 4) Failure analysis of the interfaces (determination of where the failure occurred).[31]

## 1.2.1 Adhesives and Factors Affecting Adhesion

According to the Encyclopedia of Polymer Science and Technology, "an adhesive is a material that is used to join two objects through non-mechanical bonding." [32] The adhesive is applied between the two substrates that are to be adhered. Depending on the adhesive, application of the adhesive, and the substrates the process can take advantage of any of the adhesion categories previously discussed: physical, chemical or mechanical. There are five theories of adhesion: 1) electrostatic theory, 2) diffusion theory, 3) mechanical interlocking theory, 4) acid-base theory (sometimes called specific adhesion/interaction theory), and 5) covalent bond theory. These theories are used to explain the mechanisms of adhesion. [32] It is important to note that adhesives can, and many times do, use multiple theories to maximize adhesion; for instance when using an adhesive to bond a polymer to a metal surface it is likely that the adhesive will use covalent bond theory when bonding to the polymer and electrostatic theory along with mechanical interlocking theory when bonding to the metal. Diffusion theory and acid-base theory will no longer be discussed, as they do not play a major role in this study.

There are multiple factors that affect adhesion including: 1) interactions between the adhesives and substrates (the adhesive theories that are being used in the process), 2) the surface area over which the materials are in contact, which is also known as wetting ability of the adhesive, 3) adhesive thickness, 4) and surface preparation of the substrate.

### 1.2.1.1 Electrostatic Theory

Electrostatic theory takes advantage of electron-rich ($\delta^-$) and electron-poor ($\delta^+$) sites found in functional groups throughout chemistry. This is commonly found when adhering an organic material to a metal surface as shown in **Figure 7**.
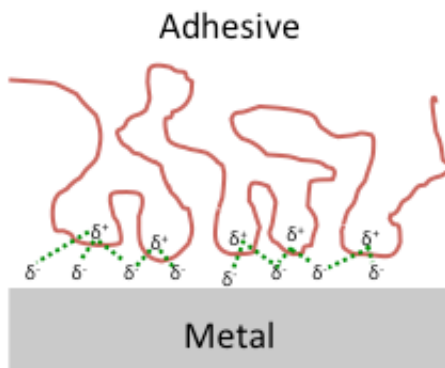


**Figure 7**: Diagram of Electrostatic Theory

The electron rich surface of the metal adheres to the electron poor sites of the adhesive creating what is known as an electrical double layer (EDL). [33,34] The resulting coulombic attraction, the attraction between the different partial charges can be seen in **Equation 1** where F is the force of attraction, k is known as Coulomb's constant, $q_1$ and $q_2$ are the charges of the two particles and r is the distance between the charged particles. [35,36]

<div align="center">**Equation 1**: Coulomb's Law</div>

$$F = k\frac{q_1 q_2}{r^2}$$

It can be seen from **Equation 1** that increasing the distance of the particles can be detrimental to the adhesive force as it is inversely proportional to the square of the distance between the charges.

## 1.2.1.2 Mechanical Interlocking Theory

Mechanical interlocking theory is said to be used when it is believed that good adhesion only comes from the adhesive penetrating the surfaces of the substrates and into the different micro crevices often found when looking at the surface of the substrate as shown in **Figure 8**.[37]  Factors such as wetting (Section 1.2.2) and rheology (the study of material flow) of the adhesive are especially important in order to have adequate adhesion.
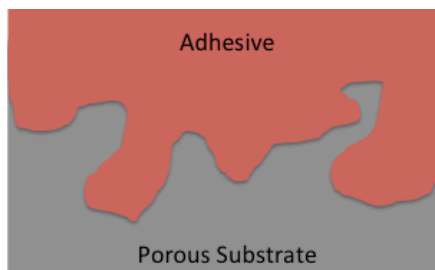


**Figure 8**: Cross-section of a magnified surface showing Mechanical Interlocking Theory

There are multiple chemical and mechanical methods that can be performed on substrates to improve the mechanical interlock.  The most common chemical method for a metal substrate is the use of a strong oxidizing agent to etch the

surface of the material. The most common mechanical method is grit blasting the material to roughen the surface.[38]

### 1.2.1.3    Chemical Bonding and Covalent Bonding Theory

Chemical Bonding is a very broad and somewhat controversial theory in regards to what sort of interactions it includes. Some authors claim that chemical bonding only includes adhesives that break and form new bonds[28,30,32] ie. covalent bonds, whereas others claim that it also includes bonds that have strong attraction for one another[36,39] ie. hydrogen bonding. No matter what types of bonds are included it can easily be agreed upon that if the strongest bond is desired it would be much better to apply primary bonds when possible due to the higher bond dissociation energies for primary bonds, **Table 1**.

**Table 1**: Typical Bond Dissociation Energies for Various Types of Bonds.[36,39,40]

| Bond Type | | Bond Dissociation Energy (kJ/mol) |
|---|---|---|
| Primary Bonds | Ionic | 700-4000 |
| | Covalent | 200-1000 |
| Secondary Bonds | Ion-dipole | 10-50 |
| | Dipole-dipole | 3-4 |
| | London dispersion | 1-10 |
| | Hydrogen Bond | 10-40 |

Many of the industrially important chemically bonding adhesives are polymer-based including: epoxy, polyurethane, and polymeric siloxanes, and resins such as

urea-formaldehyde and phenolic. The use of polymer-based adhesives allows the design of many exotic systems to allow adhesion to theoretically any substrates.[32] For instance, the adhesive used to bond the many veneers in plywood is a urea-formaldehyde resin and epoxy adhesives are used in electronics.[41,42] **Scheme 6** is a good example showing the use of secondary bonds initially and the eventual formation of primary bonds by showing adhesion between a substrate and a polymeric silane cement.

**Scheme 6**: The adhesion between a substrate and polymeric silane adhesive.[43]
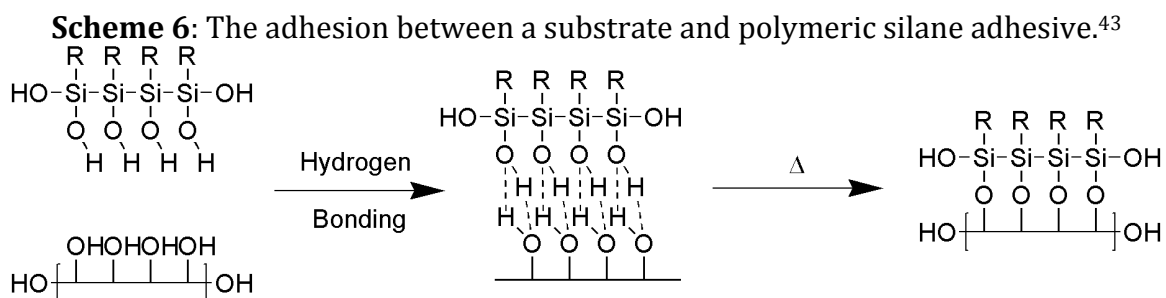


As the adhesive interacts with the surface of the metal the immediate interaction is hydrogen bonding between the hydroxyl functional groups of the metal and those of the silane. After proper wetting of the substrate, the adhesive is cured to the substrate generating the covalent bond and expelling water.

**1.2.2 Adhesive Wetting**

Wetting is known as the degree at which a liquid interacts with a surface.[44] In **Figure 9**, the wetting ability of a liquid adhesive is shown on a solid substrate.
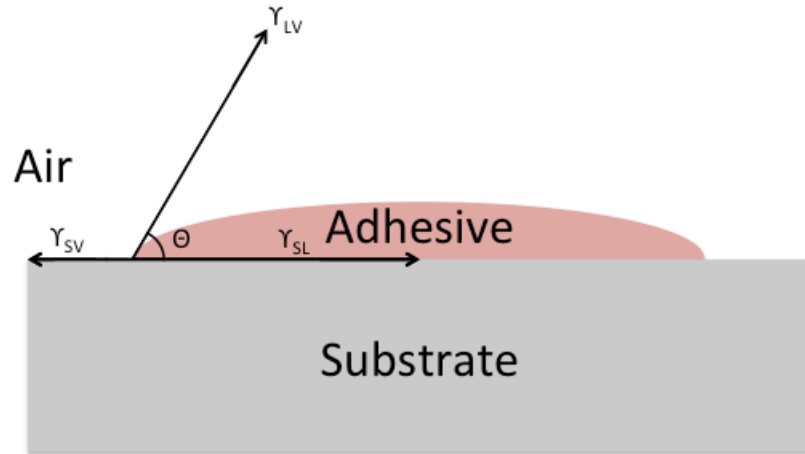
**Figure 9:** Schematic of the tension at the different interfaces between a solid and liquid. The subscripts "S", "L", and "V" stand for solid, liquid, and vapor, respectively.

The contact angle ($\theta$) of the adhesive on the substrate can be related to the individual tensions at the interface using the well-known Young-Dupré equation, **Equation 2**.[28-31,44-47]

**Equation 2**: Young-Dupré Equation.
$$\Upsilon_{SV} = \Upsilon_{SL} + \Upsilon_{LV} \cos \theta$$

There are multiple ways to manipulate the equation, but the ideal case in regards to adhesion would be complete wetness, meaning the adhesive has the ability to completely spread over the substrate. This occurs when $\Theta$ is zero or $\cos(\Theta)$ is one. Understanding this, **Equation 2** can be manipulated as shown in **Equation 3**.[28-31,44-47]

**Equation 3:** Manipulation of the Young-Dupré Equation for complete wetting.
$$\frac{\Upsilon_{SV} - \Upsilon_{SL}}{\Upsilon_{LV}} = \cos \theta = 1$$

It can be seen in **Equation 3**, that in order for complete wetting to occur the interfacial tension between the air and adhesive must be equivalent to that of the

18

difference of the interfacial tensions between that of the substrate and air and that of the substrate and adhesive. These values are specific to the substances used at the interfaces and can be manipulated by different pretreatment methods. Examples of ways to increase and decrease the interfacial tension of water on a substrate can be seen in **Table 2**.

**Table 2:** Common methods to manipulate interfacial tensions of water on a generic substrate.[46]

|  | **Increase Tension** | **Decrease Tension** |
|---|---|---|
| $\Upsilon_{LV}$ | --- | Use Surfactant |
| $\Upsilon_{SL}$ | Hydrocarbon Coating | Use Surfactant |
| $\Upsilon_{SV}$ | Plasma treatment | Hydrocarbon Coating |

### 1.2.3 Metal Preparation

The surface of received metal, although sometimes appearing clean can actually be contaminated with numerous substances that can be harmful to the substrate-adhesive interface. **Figure 10** is an illustration showing some of the possible contaminants on the surface of a metal substrate.[48] Surface contaminants are not always visible to the naked eye so pretreatment considerations should be made for all types of contamination.
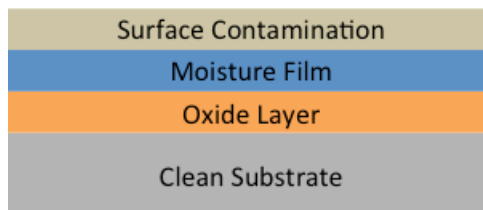


**Figure 10**: Possible contaminant layers on a metal substrate.

There are multiple methods for metal preparation. They are generally categorized as: surface preparation, surface pretreatment, and surface post-

treatment.[48]  As discussed by multiple groups, a key factor is the cleanest possible

surface for the adhesive to adhere to the substrate.[29,31,32,36,44,48]

The three general preparation methods are used to optimize adhesion by

removing specific contaminants.  The surface preparation is typically used to

improve (or allow) mechanical adhesion by grit blasting or a chemical etching

procedure.  These methods are known to easily remove oxide layers and allow for a

rough surface for adhesion.  Surface pretreatment is typically used in an attempt to

remove surface contamination (processing oils, oils from skin).  **Table 3** shows

generic surface pretreatment solvents and their ability to remove common surface

contamination.

**Table 3**: Generic Solvents to remove possible Surface Contaminants: 1 represents
poor removal, 2 represents moderate removal and 3 represents good removal. [48]

|  | Hydrocarbons | Alcohols | Esters/Ketones |
|---|---|---|---|
| **Silicone Oil** | 1 | 1 | 1 |
| **Adhesives** | 1 | 1 | 3 |
| **Fingerprints** | 1 | 3 | 3 |
| **Waxes** | 3 | 1 | 1 |
| **Protective Oils** | 3 | 1 | 3 |
| **Cutting Oils** | 2 | 1 | 3 |
| **Resins** | 3 | 3 | 3 |
| **Lubricants** | 3 | 1 | 3 |

Surface post-treatment is used to improve adhesion to the substrate and can

also aid in protecting the surface.  These are usually chemicals such as primers,

surfactants, adhesion promoters, and activators that aid by changing the interfacial

tensions to improve wetting as well as adhesion.

### 1.3    Project Introduction

The overall purpose of this project is to study the adhesion of peroxide cured FKM rubber (**Figure 1** and **Figure 5**) to cold rolled steel.  As previously discussed, FKM rubber is an extremely desirable rubber for high temperature applications due to the chemical and temperature resistance of the bulk material.  Although the relative chemical inertness is useful with many solvents it makes it difficult for peroxide cured FKMs to create a strong bond with cold rolled steel using adhesives. This project was designed to understand the role of the adhesive in the bond between metal and steel and to optimize it.

### 1.3.1   Chemical Adhesion of FKM Rubber to Steel

The first area to study was the adhesion between the adhesive and the rubber as well as the adhesive and the steel.  As discussed before, the elastomer used, PVTEM, is a peroxide cured FKM so it stands to reason that in order for the FKM to cure well to the adhesive that the adhesive must also be susceptible, at least in part, to peroxide curing.  The adhesive must also be designed to be susceptible to cure to metal.  One of the ways an adhesive can be designed to bond to the metal surface is the introduction of hydroxyl groups in the adhesive to hydrogen bond to the hydroxyl groups present on metal surface as shown in **Scheme 6**. [43,48,49]

There are many reasons for the production of polymeric silanes for adhesive purposes.  They are hybrid molecules, which can possess both organic and inorganic substituents, and are thermally stable. It has been proposed that they are

hydrolysable allowing the bonds to break and reform allowing a stress relaxation, which in turn yields stronger adhesion. [43,50,51] The majority of adhesives used in this project are polymeric silanes functionalized with various substituents.

### 1.3.2 Failure Analysis

Failure analysis is one of the most important areas when determining adhesion. The failure analysis can reveal the weakest interface of the adhesive by determining the locus of failure. **Figure 11** shows a cross-section of the adhesive interface bonded to both the rubber and the metal.
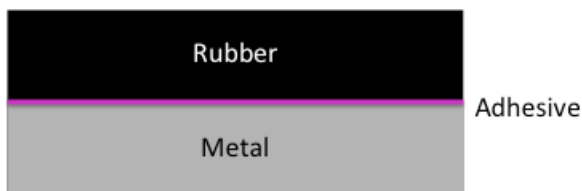


**Figure 11**: Cross-section of rubber bonded to metal using an adhesive.

The locus of failure or the interface at which the break occurs may be located in a number of places: Cohesive Rubber Failure (CRF), Rubber to Adhesive Failure (RAF), Metal to Adhesive Failure (MAF), or Cohesive Adhesive Failure (CAF). RAF occurs when the adhesive does not adequately bond to the rubber or other improper processing of the adhesive such as: dilution, mixing, application, or contamination. MAF occurs for multiple reasons such as: surface contamination to the metal, incomplete cure, and oxidized metal surface. CAF occurs when the adhesive layer is too thick causing the layer to be the weakest point in the bond. CRF is the ultimate goal of the project. CRF signifies that the adhesive bonds well enough to the metal and rubber that the rubber becomes the locus of failure.

### 1.3.3  Project Overview

The goal of this project is to develop a process that chemically adheres PVTEM, to cold rolled steel using adhesives that are known to bond to FKM rubber, supplied from Lord Chemical including: Lord Saturated Polymeric Silane  (SPS-L), Lord Unsaturated Polymeric Silane (UPS-L), Lord Unsaturated Polymeric Silane with Phosphonium Salt (UPSP-L), and Lord Phenolic Resin 1 (PR-L) and those supplied from the Dow Chemical Company: Dow Unsaturated Polymeric Silane with Phosphonium Salt 1 (UPSP-D), Dow Unsaturated Polymeric Silane 1(UPS-D1), Dow Unsaturated Polymeric Silane 2 (UPS-D2), and Dow Unsaturated Polymeric Silane 3 (UPS-D3).

The specific aims of this project are to: 1) study the insert preparation methods in order to determine their effect on the bonding between the adhesive and the insert, 2) identify and categorize the cements and determine the effectiveness of the adhesion of the cement to the rubber and the insert, 3) evaluate the components in the rubber formulations to determine if they have a positive or negative impact on the adhesive-rubber interface, and 4) identify and utilize the optimal analytical methods for determining the effectiveness of the adhesive, rubber, and insert combinations.

The approach used for gathering this information is to first find a suitable combination of insert, rubber and adhesive that yields 100% rubber cohesive failure.  This formulation can then be adjusted to determine either a positive or negative effect by changing ingredients in the rubber formulation or of the steel insert.

## 2. Experimental

### 2.1 Materials

Elastomers as well as curatives were purchased from Dupont. Carbon black was purchased from Cancarb limited. Treated Silica was purchased from Aerosil. Carnauba wax was purchased from Science Lab and *N*-octadecylamine was purchased from AkzoNobel. The TAIC was purchased from Chemtrec and *N*-(1,3-dimethylbutyl)-N'-phenyl-p-phenylenediamine was purchased from Akrochem.

### 2.2 Instrumentation

$^1$H, $^{13}$C, $^{29}$Si Nuclear Magnetic Resonance (NMR) spectra were acquired using a Bruker AVANCE 300 MHz instrument operating at 300, 75.5, and 59.6 MHz, respectively. Samples were dissolved in an appropriate deuterated solvent (DMSO-$d_6$ or Acetone-$d_6$) at a concentration of ($\sim$ 30 mg / 0.7 mL). Size Exclusion Chromatography (SEC) analysis was performed using a system consisting of a Viscotek Model 270 Dual Detector (viscometer and light scattering) and a Viscotek Model VE3580 refractive index detector. Two Polymer Laboratories 5 μm PL gel Mixed C columns (heated to 35 $^o$C) were used with a solution of 5% acetic acid in tetrahydrofuran as the eluent and a Thermoseparation Model P1000 pump operating at 1.0 mL/minute. Number average molecular weights, $M_n$, and the

dispersity were determined with the RI signal (calibrated with polystyrene standards). Unless otherwise stated, rheological profiles were acquired using a Monsanto Rheometer MDR 2000E over a six-minute window at a constant temperature of 180°C. A Varian 610-IR FT-IR Microscope was used to collect all IR data. A Tuttnauer EZ10 was used to clean the inserts by utilizing a standard glassware program, which consisted of a 30 minute sterilization at 121°C followed by a slow exhaust: 15-20 minutes.

Rubber ingredients were mixed in a Banbury Mixer 45709 for up to 15 minutes by first mixing all ingredients except PVTEM and 2,5-Dimethyl-2,5-di(t-butylperoxy)-hexane. After the other ingredients were thoroughly mixed the mixture was allowed to cool to room temperature. The 2,5-Dimethyl-2,5-di($t$-butylperoxy)-hexane was added to the mixture in a Kobelco Stewart Bolling Roller and rolled for approximately 20 minutes.

## 2.3    Standard Adhesion Test

ASTM D429 Method C - Measuring Adhesion of Rubber to Metal with a Conical Specimen was used to build the final adhesion insert (AI) as shown in **Figure 12**. The metal inserts consisted of the conical specimen seen in **Figure 13**. The AI was then pulled on an Instron 5655 at 2" per minute until break.
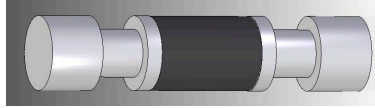
**Figure 12**: Steel AI adhered to cured Rubber.
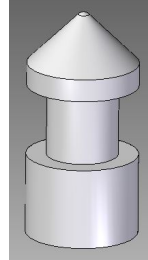


**Figure 13**: Conical Specimen.

### 2.3.1 Rubber Mixing

All rubber formulations were based off three unique rubber formulations: standard peroxide cure, bisphenol cure and combi-cure. The ingredients for the standard formulations can be seen in **Table 4**. The ingredients were added in a concentration of parts per hundred parts of elastomer, a unit that is abbreviated PHR. Typical batches were made to be ~5 lbs. Additional formulations will be shown in the Results and Discussion section.

**Table 4**: Ingredients for the three standard formulations. All subsequent formulations are based on one of these formulations.

| Formulation | Standard Peroxide Cured (SPC) | Bisphenol Cured (BPC) | Combi-cured (CC) |
|---|---|---|---|
| Ingredient | PHR | PHR | PHR |
| PVTEM-1 | 60 | | 60 |
| PVTEM-2 | 40 | | 40 |
| Poly(vinylidenefluoride-co-hexafluoropropene)-1 | | 80 | |
| Poly(vinylidenefluoride-co-hexafluoropropene)-2 | | 20 | |
| Carbon Black | 5 | 25 | 5 |
| Treated Silica | 10 | 5 | 10 |
| Calcium Hydroxide | 1.5 | 3 | 3 |
| Magnesium Oxide | 3 | 15 | 15 |
| Carnauba Wax | 0.5 | 0.5 | |
| N-octadecylamine | 1 | | |
| Sulfolane | | 0.5 | |
| N-(1,3-dimethylbutyl)-N'-phenyl-p-phenylenediamine | 0.25 | | 0.5 |
| Zinc Dimethacrylate | | | 3 |
| Triallyl Isocyanurate | 3 | | 3 |
| Benzyltriphenylphosphonium chloride | | 1.8 | |
| 4,4'-[2,2,2-Trifluoro-1-(trifluoromethyl)ethylidene] diphenol | | 3 | |
| 2,5-Dimethyl-2,5-di(t-butylperoxy)-hexane | 2.5 | | 2.5 |

## 2.3.2 Substrate

Conical specimens made of steel and brass were purchased from Stadco Automatics.

Various pretreatment methods to clean the inserts were used throughout the study and the pretreatment depended on the metal and will be further discussed in the discussion.

## 2.3.3 Adhesives

The adhesives supplied from Lord Chemical were: Lord Saturated Polymeric Silane  (SPS-L), Lord Unsaturated Polymeric Silane (UPS-L), Lord Unsaturated Polymeric Silane with Phosphonium Salt (UPSP-L), and Lord Phenolic Resin 1 (PR-L).    Those supplied from the Dow Chemical  Company    include:   Dow

Unsaturated Polymeric Silane with Phosphonium Salt 1 (UPSP-D), Dow Unsaturated Polymeric Silane 1(UPS-D1), and Dow Unaturated Polymeric Silane 2 (UPS-D2).

### 2.3.3.1    Adhesive Dilution

Three representative adhesives were used for the adhesion tests: UPSP-D, UPS-L, and SPS-L. The adhesives were diluted to have roughly the same dry solid content using solvents recommended by the supplier.  UPSP-D was diluted one part adhesive per three parts of ethanol, UPS-L was diluted one part adhesive per two parts ethanol and SPS-L was diluted one part adhesive per one part water.

### 2.3.3.2    Adhesive Application

Adhesive was applied to the inserts by either a dipping method or spraying method.  The dipping method involved complete submersion of a clean insert in the adhesive; it was immediately removed and allowed to air dry.  The spraying method involved spraying the adhesive on the insert with an Ingersoll-Rand Model 270G paint sprayer. The coated inserts were stored overnight in a dry, enclosed area.

### 2.3.4  Molding

After mixing the rubber, and preparing the inserts, four prepared inserts (**Figure 13**) were loaded into the mold cavity as shown in **Figure 14**.  Roughly 40 g of rubber was loaded into the transfer pot.  The rubber and inserts were then molded in a Wabash 50-1212-2TM press at a pressure of ~2600 PSI and temperatures ranging from 150°C to 190°C although 180°C-190°C for four to six minutes was typically chosen.   Hot   transfer molding was utilized, **Figure 15**.
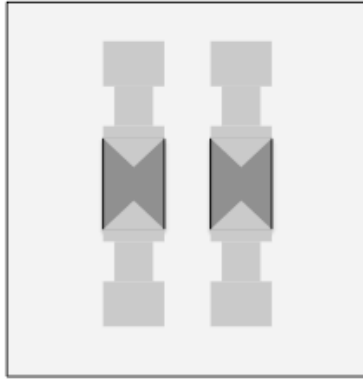
**Figure 14**: Top View of Open Mold Cavity.
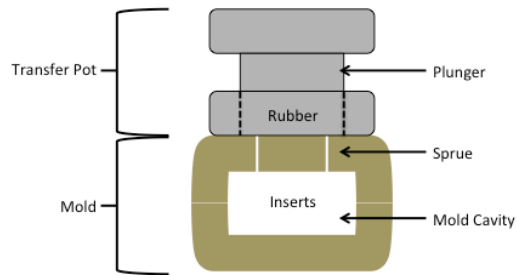


**Figure 15**: Hot Transfer Diagram

This process yielded two adhesion inserts (AIs), **Figure 12**, that were allowed to cool overnight before pulling the AI.

### 2.3.5  Failure Testing

Four AIs were used for each test.  The AIs were pulled using an Instron 5655 extensometer at a constant rate of 2" per minute until the specimen broke.  The software generated a plot of load (lbf) vs. extension (in), **Figure 16.**
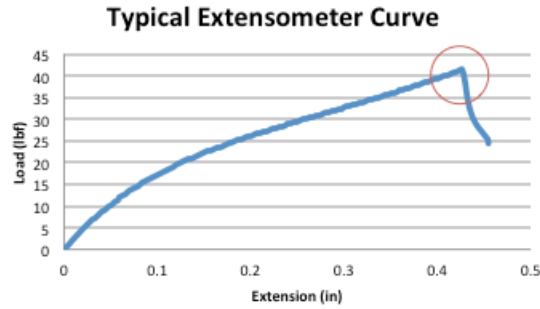
**Figure 16**: Typical Extensometer Curve.

The maximum load the AI endured was the desired datum of the plot (area circled in red in **Figure 16**).

### 2.3.6  Rubber Retention

The rubber retention was measured using a subjective method of determining the amount of rubber that remained on the AI after break.  The method used a scale from zero to five.  A value of zero was assigned to AI's that had complete failure at the interface.  These parts exhibited rubber-to-adhesive failure (RAF), metal-to-adhesive failure (MAF), or cohesive adhesive failure (CAF).   A value of five was assigned to AI's that showed cohesive rubber failure (CRF).

### 2.4    Various Experiments

### 2.4.1  Rubber

### 2.4.1.1      Blended Coagent Study

The peroxide cured FKM with the following coagents:  Zinc Dimethacrylate, *N*-(1,3-dimethylbutyl)-*N*'-phenyl-*p*-phenylenediamine, and Triallyl Isocyanurate.  This was examined by adding coagents to a    master batch to make seven small-scale

batches (A-G).  **Table 5** shows the ingredients used to make batches A-G.

**Table 5**: Blended Coagent Study.  Seven different combinations of coagents were added to the master batch.  The total amount added is shown in the table.  Gray boxes represent no change for the particular ingredient from the master batch.

| Formulation | Master Batch | A | B | C | D | E | F | G |
|---|---|---|---|---|---|---|---|---|
| Ingredient | PHR | PHR | PHR | PHR | PHR | PHR | PHR | PHR |
| PVTEM-1 | 60 | | | | | | | |
| PVTEM-2 | 40 | | | | | | | |
| Carbon Black | 5 | | | | | | | |
| Treated Silica | 10 | | | | | | | |
| Calcium Hydroxide | 1.5 | | | | | | | |
| Magnesium Oxide | 3 | | | | | | | |
| Carnauba Wax | 0 | | | | | | | |
| N-octadecylamine | 0 | | | | | | | |
| N-(1,3-dimethylbutyl)-N'-phenyl-p-phenylenediamine | 0 | | | 1 | 1 | 1 | 0.5 | 0.5 |
| Zinc Dimethacrylate | 0 | 2 | | 2 | 3 | 2 | 3 | 2 |
| Triallyl Isocyanurate | 3 | | 5 | | | 4 | | 4 |
| 2,5-Dimethyl-2,5-di(t-butylperoxy)-hexane | 2.5 | | | | | | | |

After mixing batches A-F, a rheological profile was gained using a Monsanto Rheometer MDR 2000E at 180°C over a six-minute window.

## 2.4.1.2        Cure Determination by Swelling Data

An extended rheology plot was made by curing the material at 150°C for 60 minutes. A calibration curve was generated using the extended rheology plot and **Equation 4**, where $M_H$ is the upper limit of the plot and $M_L$ is the lower limit and TC is the theoretical cure.

**Equation 4**: Equation to determine the torque at various theoretical cures.
$$(M_H - M_L) \times TC + M_L = \text{Torque at TC}$$

Square test slabs were made using the previously mentioned press fitted with a square mold (6" x 6" x 0.075").  The press was set to 150°C and rubber was allowed to cure for these amounts of time: 4 minutes 40 seconds, 8 minutes 55 seconds, 14 minutes 30 seconds, 24 minutes 6 seconds, and 41 minutes 36 seconds for theoretical cures of 10, 30, 50, 75   and 95%, respectively.   The test slabs

31

were immediately quenched with ice water. Three small discs were cut from each test slab (about 1" diameter) and weighed (Weight$_{initial}$). After obtaining the weight of each the discs were immersed in an enclosed solution of methyl ethyl ketone for 3 days and stored at room temperature. The discs were removed from the solution and weighed again (Weight$_{swell}$). After determining the swell weight the discs were allotted 24 hours to dry at room temperature and then heated in an oven at 100$^{o}$C for 2 hours, followed by weighing to determine a dry weight (Weight$_{dry}$). The %Swell was calculated using **Equation 5**.

**Equation 5**: Equation to determine %Swell.

$$\%\text{Swell} = \left(\frac{\text{Weight}_{\text{swell}} - \text{Weight}_{\text{dry}}}{\text{Weight}_{\text{dry}}}\right) \times 100$$

A calibration curve was generated by plotting %Swell vs. Theoretical Cure. The calibration curve (**Figure 17**) yielded an $R^2$ value of 0.993.
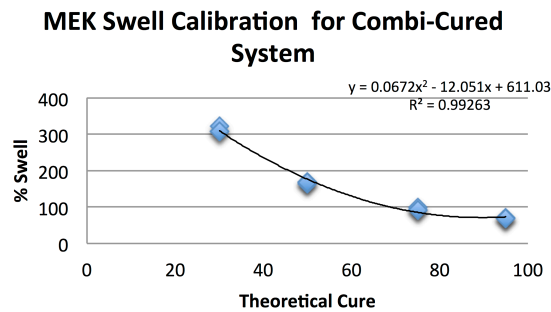


**Figure 17**: Methyl ethyl ketone swell calibration curve. The data was run in triplicate.

The data on individual AIs were gained by gathering the residual plugs from the sprue in the molding apparatus. The plugs underwent the same swell conditions

and the %Swell was calculated.

### 2.4.1.3    Adhesion at Theoretical Cures

The method used in **Cure Determination** was modified to determine the actual cure versus time in the mold.  Inserts coated with UPSP-D were molded at $150^oC$ for the times that would yield 10, 30, 50, 75 and 95% cure.  Methods **Failure Testing** and **Rubber Retention** were used to pull the AI and determine rubber retention, respectively.

### 2.4.2  Adhesive

### 2.4.2.1    Adhesive Categorization

Adhesive characterization was performed using $^1$H NMR spectroscopy operating at 300 MHz, with samples dissolved in DMSO-$d_6$.  SPS-L was categorized by $^1$H NMR spectroscopy (DMSO-$d_6$, $\delta$): 0.54 (bp, 2H), 1.41 (bp, 2H).  UPS-L, UPS-D1, UPS-D2 were categorized by $^1$H NMR (DMSO-$d_6$, $\delta$): 0.59 (bp, 2H), 1.48 (bp, 2H), 2.57 (bp, 2H), 5.92 (bp, 2H), 6.05 (bp, 1H).  UPSP-L and UPSP-D were categorized by $^1$H NMR (DMSO-$d_6$, $\delta$): 0.59 (bp, 2H), 1.48 (bp, 2H), 2.57 (bp, 2H), 5.92 (bp, 2H), 6.05 (bp, 1H), 7.37 (m, 5H). The polymeric silane from UPSP-D was categorized by 75.5 MHz DEPT 135 $^{13}$C NMR spectroscopy (DMSO-$d_6$, $\delta$): 37.1 (2H), 48.9 (2H), and 62.6 (2H).

### 2.4.2.2    Attenuated Total Reflectance Fourier Transform Infrared Spectroscopy (ATR FT-IR)

ATR FT-IR was performed on the   adhesive    films    using    absorbance

scanning in the range from 600 to 4000 cm$^{-1}$.  Adhesives were loaded into test tubes and dried overnight in a Savant SpeedVac, which typically reached pressures around 500 millitorr and was at a constant temperature of 43$^o$C.  The remaining films were then scraped from the test tubes.

### 2.4.3  Adhesion Insert (AI)

#### 2.4.3.1        End-to-End

Attenuated Total Reflectance Fourier Transform Infrared Spectroscopy (ATR FT-IR) was used on an inverted AI (**Figure 18**) to determine the locus of failure after break.
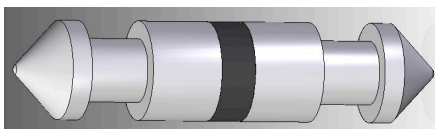


**Figure 18**: End-to-end AI.

#### 2.4.3.2        Window Dye

The window dye method allowed only half of the rubber to cure to the insert, **Figure 19**.
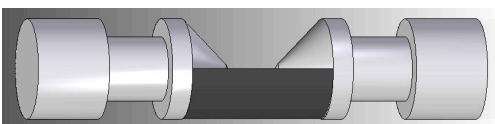


**Figure 19**: Window Dye AI.

A dye of post-cured ethylene propylene diene monomer (EPDM) rubber was molded with steel inserts that were not coated with adhesive to gain the general shape of the AI.  The rubber was then cut in half vertically and post-cured at 200$^o$C for 16 hours, **Figure 20**.

34
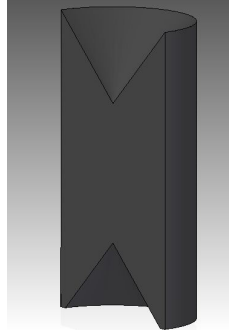
**Figure 20**: Window Dye Piece.

The cut dye was inserted into the bottom of the mold and the AI was formed in the typical fashion, yielding the part shown in **Figure 19**.

The AI was pulled at 2" per minute and video was recorded using a digital camera on an iPhone 5.

### 2.4.4  Design of Experiments

### 2.4.4.1        Metal Pretreatment Design of Experiment (DOE)

The pretreatment DOE was designed to have five variables: two solvent rinses, use of an autoclave, the use of grit blasting and flashing off the solvents after the adhesive was applied.  Again the pretreatment DOE was designed to have five variables, two levels (on or off), and 16 experiments.  The 16 experiments are shown in **Table 6**.

**Table 6**: Metal Pretreatment DOE.

| Run Order | 1st Solvent Rinse | Autoclave | Grit Blast | 2nd Solvent Rinse | Solvent Flash |
|-----------|-------------------|-----------|------------|-------------------|---------------|
| 1 | -1 | 1 | 1 | -1 | 1 |
| 2 | -1 | -1 | 1 | -1 | -1 |
| 3 | 1 | 1 | 1 | 1 | 1 |
| 4 | -1 | -1 | -1 | -1 | 1 |
| 5 | -1 | 1 | -1 | 1 | 1 |
| 6 | 1 | -1 | 1 | 1 | -1 |
| 7 | -1 | -1 | -1 | 1 | -1 |
| 8 | 1 | -1 | -1 | 1 | 1 |
| 9 | -1 | -1 | 1 | 1 | 1 |
| 10 | 1 | 1 | -1 | -1 | 1 |
| 11 | 1 | 1 | -1 | 1 | -1 |
| 12 | 1 | -1 | 1 | -1 | 1 |
| 13 | -1 | 1 | 1 | 1 | -1 |
| 14 | 1 | 1 | 1 | -1 | -1 |
| 15 | 1 | -1 | -1 | -1 | -1 |
| 16 | -1 | 1 | -1 | -1 | -1 |

The use of "1" in **Table 6** indicates use of the pretreatment and "-1" indicates skipping the selected pretreatment. First and second order relationships were calculated and an equation was developed to determine the optimal combination of pretreatments to use in order to yield maximum adhesion to steel and maximum tensile stress at break.

## 2.4.4.2    Formulation Design of Experiment (DOE)

The formulation DOE was designed to have five variables: carbon black, treated silica, carnauba wax, *N*-octadecylamine, and zinc dimethacrylate, two levels (on or off), and 16 experiments. The 16 experiments are shown in **Table 7**.

**Table 7**: Formulation DOE Experiments

| Run Order | Carbon Black | Treated Silica | Carnauba Wax | N-Octadecyl amine | Zinc Dimethacrylate |
|-----------|--------------|----------------|--------------|-------------------|---------------------|
| 1 | -1 | 1 | 1 | -1 | 1 |
| 2 | -1 | -1 | 1 | -1 | -1 |
| 3 | 1 | 1 | 1 | 1 | 1 |
| 4 | -1 | -1 | -1 | -1 | 1 |
| 5 | -1 | 1 | -1 | 1 | 1 |
| 6 | 1 | -1 | 1 | 1 | -1 |
| 7 | -1 | -1 | -1 | 1 | -1 |
| 8 | 1 | -1 | -1 | 1 | 1 |
| 9 | -1 | -1 | 1 | 1 | 1 |
| 10 | 1 | 1 | -1 | -1 | 1 |
| 11 | 1 | 1 | -1 | 1 | -1 |
| 12 | 1 | -1 | 1 | -1 | 1 |
| 13 | -1 | 1 | 1 | 1 | -1 |
| 14 | 1 | 1 | 1 | -1 | -1 |
| 15 | 1 | -1 | -1 | -1 | -1 |
| 16 | -1 | 1 | -1 | -1 | -1 |

The "1" indicates using the specific ingredient and "-1" indicates completely omitting it. When included, the amounts used were: 5 PHR, 10 PHR, 0.5 PHR, 1 PHR, and 3 PHR for carbon black, treated silica, carnauba wax, *N*-octadecylamine, and zinc dimethacrylate, respectively. First and second order relationships were calculated and an equation was developed to determine the optimal combination of ingredients to use in order to yield maximum rubber retention to steel and maximum adhesion strength.

### 2.4.5 Locus of Failure

For this test steel inserts were used with UPSP-D. Adhesive was loaded into test tubes and dried overnight in the Savant SpeedVac, with typically reached pressures around 500 millitorr and was    at a constant temperature of 43°C. ATR

FT-IR data was collected on the UPSP-D film.

A combination of rubber and adhesive known for failure at an interface was used.  The AI was made using the end-to-end orientation and pulled using the standard 2" per minute conditions.  ATR FT-IR data were collected on both the steel insert and the rubber after the pull and compared to the UPSP-D film.

The steel insert was also sent to the University of Dayton Research Institute (UDRI) for XPS analysis.

# 3.    Results and Discussion

The results and discussion will be divided into the following sections: Adhesive Information, Rubber, Substrate and Substrate Preparation, and Locus of Failure.  The analytical methods utilized and corresponding data will be discussed concurrently.

## 3.1    Adhesive Information

Seven adhesives were categorized.  Adhesives from Lord Chemical include: Lord Saturated Polymeric Silane  (SPS-L), Lord Unsaturated Polymeric Silane (UPS-L), Lord Unsaturated Polymeric Silane with Phosphonium Salt (UPSP-L), and Lord Phenolic Resin 1 (PR-L) and those supplied from the Dow Chemical Company include: Dow Unsaturated Polymeric Silane with Phosphonium Salt 1 (UPSP-D), Dow Unsaturated Polymeric Silane 1(UPS-D1), and Dow Unsaturated Polymeric Silane 2 (UPS-D2).

### 3.1.1  NMR of Adhesives

Upon receipt, very little was known about the structure and therefore potential curing mechanisms of the suggested adhesives.  Some of the MSDS's indicated that the adhesives were based on a polymeric silane, while others were not so forthcoming with that information.

$^1$H and DEPT 135 $^{13}$C NMR spectroscopy along with IR spectroscopy were utilized to determine the structure of the polymeric silanes used as the adhesive.

39

From the data gathered it can be said with reasonable certainty that all of the adhesives seem to use hyper-branched silanes while sometimes varying the functional groups present for adhesion.

The polymeric silane from UPSP-D was extracted from the phosphonium salt by stirring in acetone. The phosphonium salt was soluble in acetone; the polymeric silane was not. The DEPT 135 spectrum was run on the polymeric silane to determine the nature of the carbon atoms. The DEPT 135 showed the presences of only methylene-type ($-CH_2-$) carbon atoms in the aliphatic region of the spectrum. To confirm these surprising data the sample was spiked with tetrahydrofuran (a compound containing only methylene-type carbon atoms). The spiked sample confirmed the presence of $-CH_2-$ groups and one CH group.

When considering this and the $^1H$ NMR data which follow, it was determined that there was likely a vinylic functional group present in some of the adhesives as well as a 3-amino propyl group present in all of the adhesives as indicated in **Figure 21**.
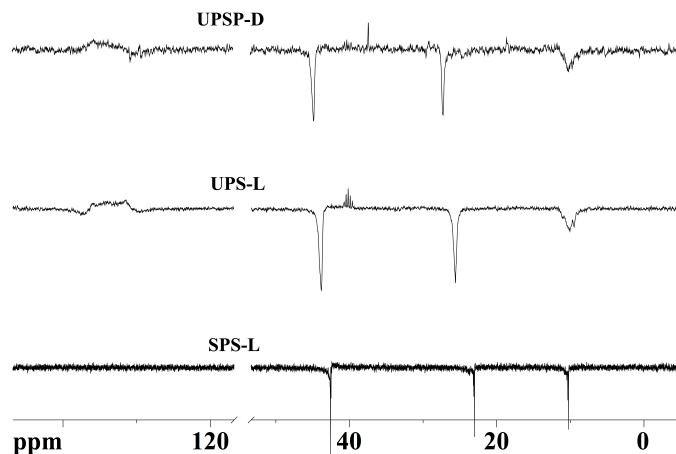
**Figure 21:** 75.5 MHz DEPT 135 NMR spectra (DMSO-$d_6$) of the polymeric silanes isolated from the three standard adhesives.

UPSP-D was slightly more challenging than the other adhesives due to the presence of the phosphonium salt. It was discovered that the phosphonium salt could be extracted from the mixture by stirring in acetone. **Figure 22** shows the dried adhesive, as well as, both the polymeric silane and phosphonium salt isolated indicating that stirring in acetone was a sufficient method to extract the phosphonium salt.
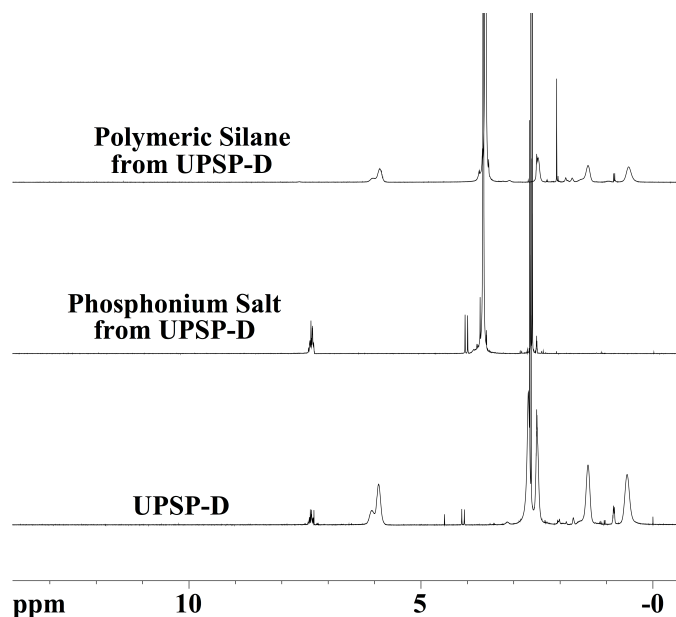
**Figure 22:** 300 MHz $^1$H NMR spectrum (DMSO-$d_6$) of overlay of polymeric silane and phosphonium salt from UPSP-D along with UPSP-D.

The 300 MHz $^1$H NMR spectrum (DMSO-$d_6$) of phosphonium salt from UPSP-D is shown in **Figure 23**. The MSDS also included the CAS no. for the phosphonium salt, 94088-77-4, which was used to determine the structure of the salt. The phosphonium salt was expected to play two roles in adhesion. The first is that quaternary phosphonium salts are known to activate steel. The second is that they are also used as a catalyst in the bisphenol curing mechanism, **Scheme 4**.
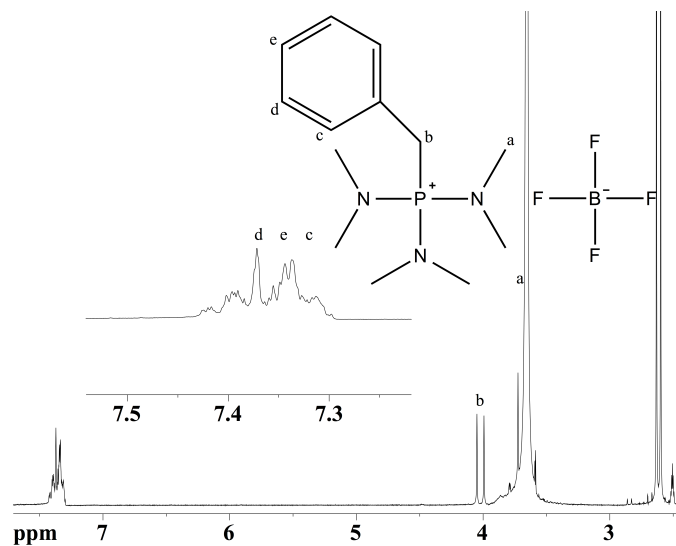
**Figure 23**: 300 MHz $^1$H NMR spectrum (DMSO-$d_6$) of phosphonium salt from UPSP-D.

The $^1$H NMR spectrum of the polymeric silane extracted from UPSP-D (**Figure 24**) shows the presence of unsaturation, likely being a vinylic side group. The presence of the vinylic group is believed to aid in radical curing.
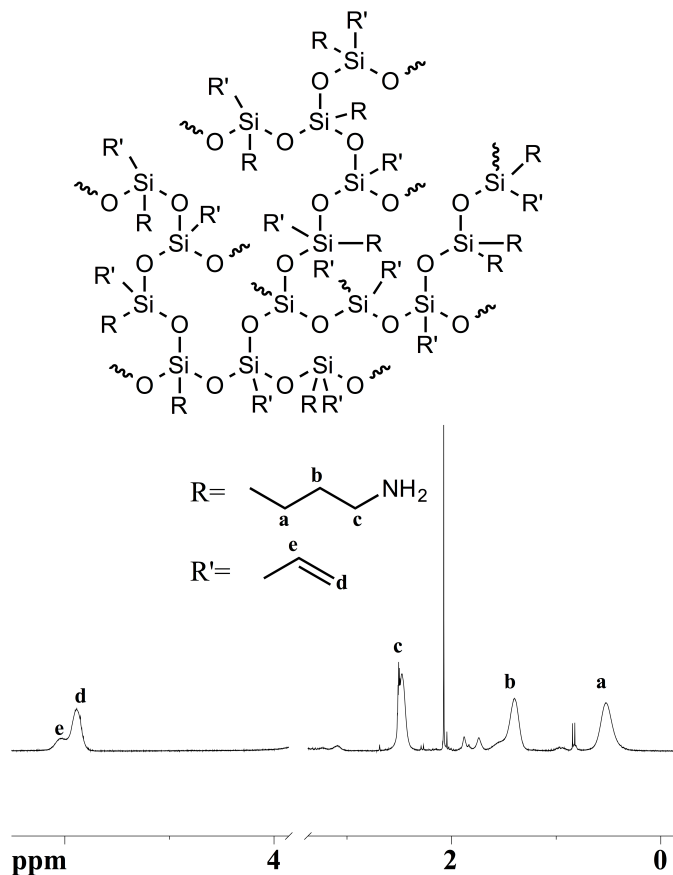
**Figure 24:** 300 MHz $^1$H NMR spectrum (DMSO-$d_6$) of polymeric silane from UPSP-D.

The $^1$H NMR spectrum of the polymeric silane isolated from UPSP-D (**Figure 24**) closely resembles that of the UPS-L (**Figure 25**) and they are believed to bond to the rubber with a similar mechanism.

The next adhesive categorized was the UPS-L. This was characterized as still being a hyperbranched polymeric silane with the amino propyl functional group, but also contained unsaturation. The unsaturation came in the form of a vinylic group, which was believed to cure well to the rubber allowing the propyl amine to bond to the steel substrate (**Figure 25**).

44
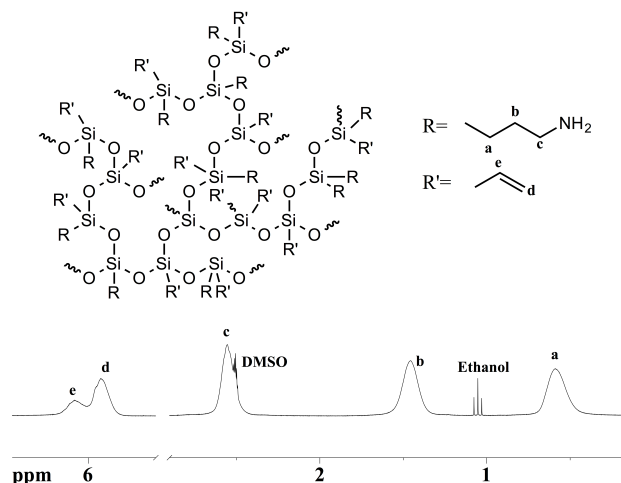
**Figure 25**: 300 MHz $^1$H NMR spectrum (DMSO-$d_6$) of Unsaturated Polymeric Silane from Lord (UPS-L).

The $^{29}$Si NMR spectrum is indicative of a hyperbranched polymeric silane that appears to have two cure sites, **Figure 26**. It should also be noted that the broad peak found around -110 ppm is common in $^{29}$Si NMR and is due to the presence of Si in the NMR glass tubing.
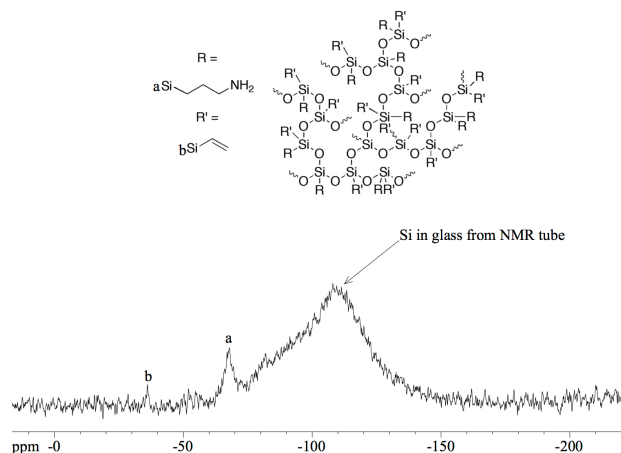


**Figure 26:** 59.6 MHz $^{29}$Si NMR spectrum (DMSO-$d_6$) of Unsaturated Polymeric Silane from Lord (UPS-L).

The next spectrum studied was of SPS-L. This polymer showed no unsaturation, was very soluble in water and was basic. This information strongly

indicated the presence of an amino functional group. From these data, along with the spectra from **Figure 27** indicating three sets of unique protons and **Figure 28** indicating the presence of one cure-site, it was believed that the polymer is a hyperbranched polymeric silane with propyl amino groups available for curing to the rubber as well as the steel.
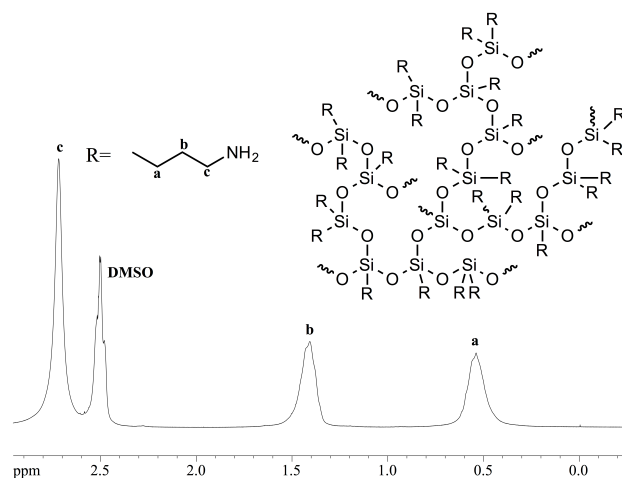


**Figure 27:** 300 MHz ¹H NMR spectrum (DMSO-$d_6$) of Saturated Polymeric Silane from Lord (SPS-L).
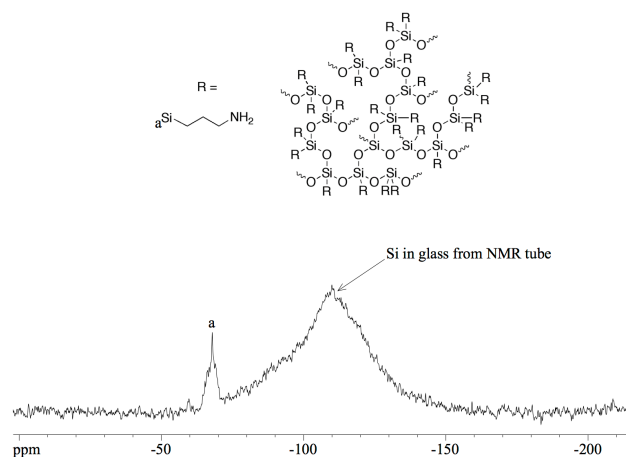
**Figure 28:** 59.6 MHz $^{29}$Si NMR spectrum (Acetone-$d_6$) of Saturated Polymeric Silane from Lord (SPS-L).

## 3.1.2 IR of Adhesives

Although a lot of evidence pointed to the presence of amino groups in these adhesives, it was not confirmed by the NMR data. ATR FT-IR spectroscopy was performed on the adhesive films. The complete spectra can be seen in **Figure 29**. Although the amino groups are still not prominent there is some evidence of a primary amino group in SPS-L. A closer look in the amino region of the IR ~3000 to ~3500 cm$^{-1}$ suggests the presence of primary amino groups in all three adhesives, **Figure 30**.
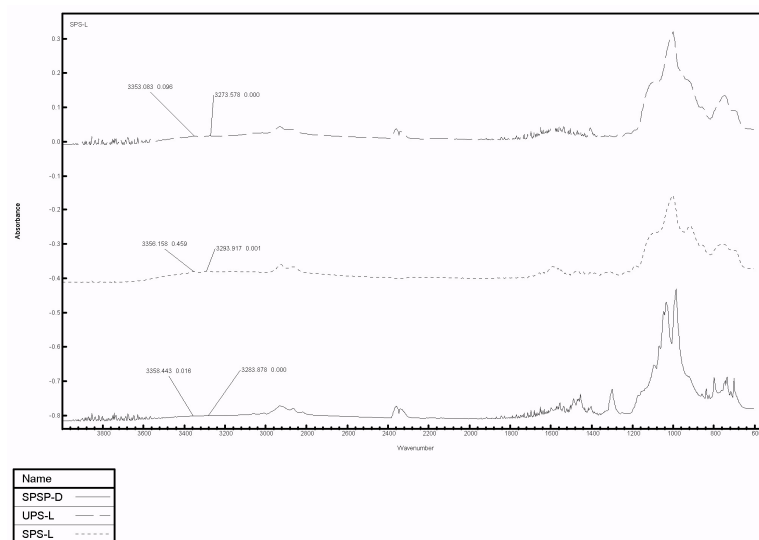
**Figure 29**: Full IR spectra of UPSP-D, UPS-L, and SPS-L.
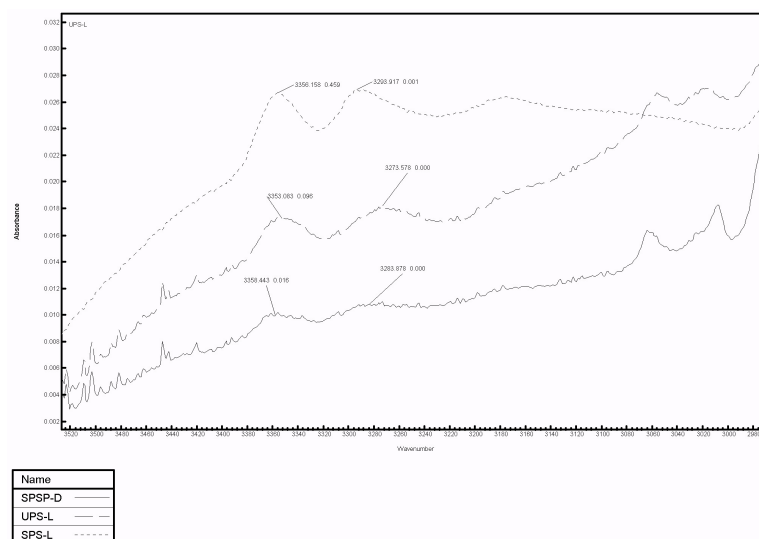


**Figure 30**: IR spectra of three sample adhesives showing amine region.

### 3.1.3 Adhesive Categorization

Adhesives were categorized by the functional groups present, as confirmed by ^{1}H, ^{13}C and ^{29}Si NMR and IR data, as well as the most likely curing mechanism to be employed. The first category was the unsaturated polymeric silanes: UPS-L, UPS-D1, UPS-D2, and UPS-D3, **Figure 31**.  These types of adhesives were believed to cure to the rubber through a radical mechanism because the unsaturation was believed to

be susceptible to radical attack. It was also believed that these polymers cured to the metal through the amino functional group present.
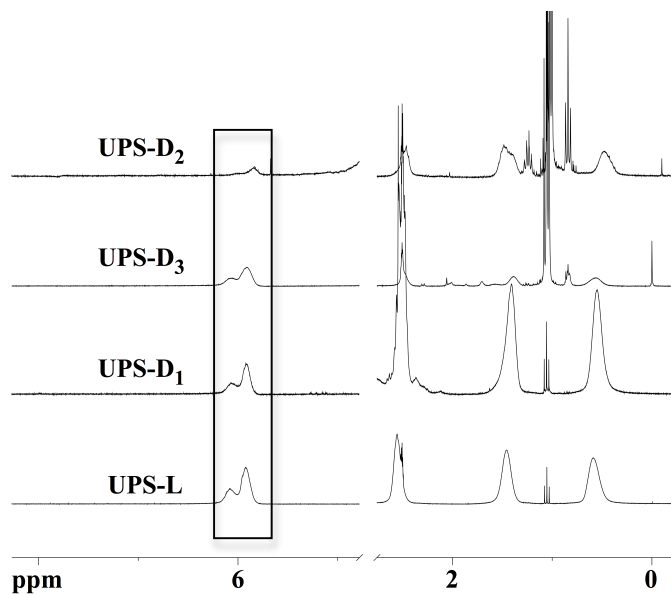


**Figure 31:** 300 MHz $^1$H NMR spectra (DMSO-$d_6$) of all unsaturated polymeric silanes.

The second category was the saturated polymeric silane. The only adhesive that fell within this category was the SPS-L. It was believed that this adhesive was only able to cure through the propyl amine functional group that is present.

The final category is the unsaturated polymeric silane with phosphonium salt, which includes: UPSP-L and UPSP-D (**Figure 32**). This group looks and is believed to act similarly to the UPS adhesives. The difference is that this group also has a phosphonium salt present that is believed to aid in curing.
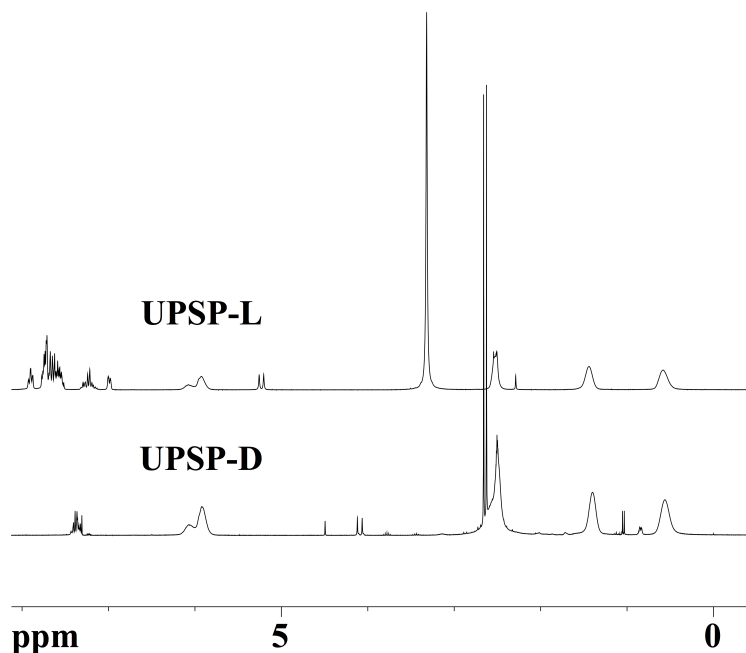
**Figure 32:** 300 MHz $^1$H NMR spectra (DMSO-$d_6$) of unsaturated polymeric silanes with phosphonium salt.

## 3.2    Rubber

### 3.2.1  Characterization of PVTEM

#### 3.2.1.1        Size Exclusion Chromatography

The two elastomer formulations that were tested: Poly[vinylidenefluoride-co-tetrafluoroethylene-co-perfluoro(methyl vinyl ether)-co-iodotrifluoroethylene] (PVTEM-1) and Poly[vinylidenefluoride-co-tetrafluoroethylene-co-perfluoro(methyl vinyl ether)-co-iodotrifluoroethylene] (PVTEM-2)  were dissolved in a solution of 5% acetic acid in THF.  The overlay containing the two elastomers can be seen in **Figure 33**.  PVTEM-1 eluted at 12.5 minutes, which corresponded to number-average molecular weight ($M_n$): 72,600 (Da), weight-average molecular weight

($M_w$): 117,400 (Da), and PDI: 1.6. PVTEM-2 eluted at 12.3 minutes, which corresponded to $M_n$: 90,400 (Da), $M_w$: 166,700 (Da), and PDI: 1.8.
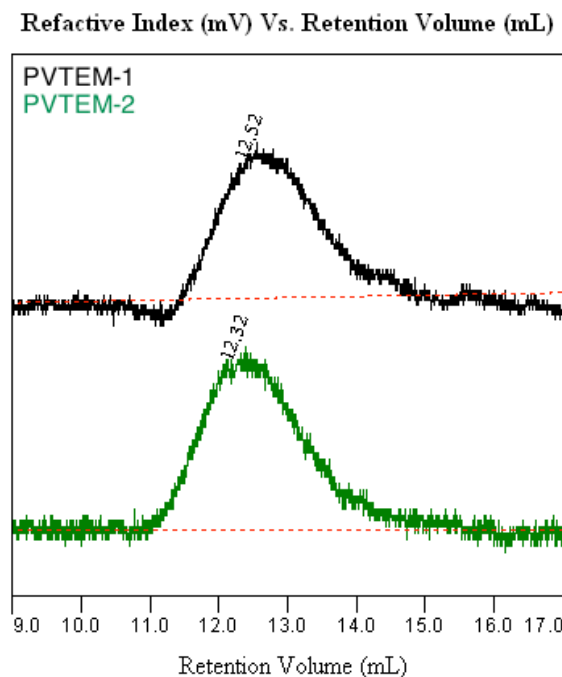


**Figure 33**: Overlay of PVTEM 1 and PVTEM 2.

### 3.2.2 Rubber Formulations

The rubber formulations fell into three specific categories based on predicted curing. The first rubber category used was the standard peroxide cured (SPC) formulation. This formulation was a starting point formulation generated to include ingredients common to peroxide cured FKM rubber formulations. The standard peroxide cured rubber formulation and additional formulations derived from SPC can be seen in **Table 8**.

**Table 8**: Ingredients in all Standard Peroxide Cured Formulations.

| Formulation | Standard Peroxide Cured (SPC) | SPC-CB+ZDMA | SPC-CB-TS | SPC-TS-CB+RT | SPC-CB+ZDMA | SPC-CW-NOA-RT | SPC-CW-NOA+RT+ZDMA | SPC-CW-NOA |
|---|---|---|---|---|---|---|---|---|
| Ingredient | PHR | PHR | PHR | PHR | PHR | PHR | PHR | PHR |
| PVTEM-1 | 60 | | | | | | | |
| PVTEM-2 | 40 | | | | | | | |
| Carbon Black | 5 | 0 | 0 | 0 | 0 | | | |
| Treated Silica | 10 | | 0 | 0 | | | | |
| Calcium Hydroxide | 1.5 | | | | | | | |
| Magnesium Oxide | 3 | | | | | | | |
| Carnauba Wax | 0.5 | | | | | 0 | 0 | 0 |
| N-octadecylamine | 1 | | | | | 0 | 0 | 0 |
| N-(1,3-dimethylbutyl)-N'-phenyl-p-phenylenediamine | 0.25 | | | 1.5 | | 0 | 1.5 | |
| Zinc Dimethacrylate | 0 | 2 | | | 3 | | 3 | |
| Triallyl Isocyanurate | 3 | | | | | | | |
| 2,5-Dimethyl-2,5-di(t-butylperoxy)-hexane | 2.5 | | | | | | | |

A ratio of 60 parts PVTEM-1 and 40 parts PVTEM-2 were the elastomers chosen for all SPC formulations. The two elastomers were chosen because they are designed to blend well and allow for a wider range of desired properties. Carbon Black (CB) and Treated Silica (TS) were added in an attempt to aid in the final physical properties of the rubber. CB also gave the cured rubber a solid black color. Calcium hydroxide and magnesium oxide were added as a source of a base for the curing mechanism to occur. Carnauba Wax (CW) and *N*-octadecylamine (NOA) are considered process aids, which aid as a mold release and mill release, respectively. They were expected to hurt adhesion but were deemed necessary in order to allow the rubber to be processed. *N*-(1,3-dimethylbutyl)-*N'*-phenyl-*p*-phenylenediamine (RT), Triallyl Isocyanurate (TAIC), Zinc Dimethacrylate (ZDMA), and 2,5-Dimethyl-2,5-di(t-butylperoxy)-hexane (DTBPH) were all necessary for the peroxide cured mechanism to work properly. RT acted as a radical trap and has been shown to retard the rate of cure. TAIC was used as a crosslinking agent, which allowed the rubber to cure properly. ZDMA, although not needed for curing, was used as an adhesion promoter because of the unique design allowing it to bond to the metal

and cure with the rubber.  DTBPH was the source of the peroxide necessary for the crosslinking mechanism.

The initial SPC formulation with UPSP-D and steel did not afford good adhesion.  It was found that there was no rubber retention (0) and that the failure was completely at the interface: CAF, MAF, or RAF.  Although this information was useful in determining that adhesion needed to improve, the locus of failure could not be determined.  The plan to solve this issue was to add a new adhesive, SPS-L, which was tagged with a phosphorescent sensor.  The experiment was repeated with SPS-L and 0 rubber retention occurred again.  The use of the phosphorescent sensor showed that the adhesive remained bonded to the steel insert, but it was not found on the rubber.

The concern was that the adhesive should have bonded well to the rubber but the dye could not be seen because the CB in the rubber essentially quenched the dye.  The concern generated lead to a new formulation of SPC without CB, but with added ZDMA (SPC-CB+ZDMA).  This formulation removed CB in hopes that the dye, if present, could be seen on the rubber and also introduced ZDMA, which was shown by Henning *et al*[52] to increase adhesion to steel.  The same failure occurred and the dye was still only present on the steel substrate.  This was the initial information that showed that the issue was the rubber formulation.

One of the original theories was that there were a limited amount of sites that were available for curing.  These sites were to either cure to one-another through crosslinks or cure to the adhesive.  Looking at the rheology, it was believed

53

that the crosslinking mechanism occurred too rapidly for the rubber to interact with the slower curing adhesive.

In order to combat this issue an increased level of RT, which acts as a retardant, was added to the mixture in order to decrease the rate of radical curing. This generated a formulation of SPC-CB-TS+RT.

The rheological profiles of SPC and SPC-CB-TS+RT are present in **Figure 34**. The increased RT drastically reduced the initial slope in the rheology trace, which was believed to give an opportunity for the adhesive to wet the polymer. The slower rate was believed to give opportunity to the adhesive to mix with the rubber before the rubber completely cross-linked.
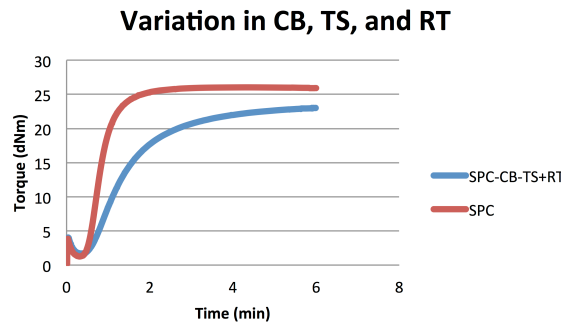


**Figure 34**: Rheology Profile of SPC and SPC-CB-TS+RT.

**Figure 35** displays adhesion data obtained from the two rubber mixtures that varied the amount of RT. Since formulation SPC-CB-TS+RT had significantly more retardant (factor of six increase) and should have allowed the mixture of adhesive and rubber the belief was that SPC-CB-TS+RT would have much greater adhesion capabilities than formulation SPC however, this was not the case. The data pointed to a couple of possibilities. The first was that even with the added retardant the radical curing was not slowed enough for wetting to occur. The other possibility

was that the opportunity to bond might not have been the only parameter required to be promote adhesion.

ZDMA as well as TS was later introduced, SPC-CB+RT+ZDMA, in that these ingredients (all believed to help adhesion) would help improve the adhesive capabilities. Again this was not the case. Formulation SPC-CB+RT+ZDMA using adhesives UPSP-D, UPS-L, and SPS-L to bond to steel still yielded 0 rubber failure.
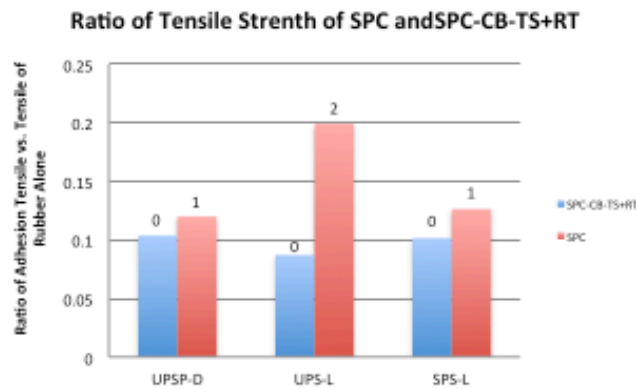


**Figure 35**: Adhesion data of SPC and SPC-CB-TS+RT. The numbers above the graphs represent average rubber failure on a subjective 0-5 scale: 0 = complete interfacial failure, 5 = cohesive rubber failure

The continued lack of success led to formulation, SPC-CW-NOA-RT, which was not used in a traditional sense, but was used to make smaller scale batches as part of a blended coagent study similar to Henning et. al. Seven different small-scale batches were formulated and their rheological profiles were determined (**Figure 36**). The coagents added to SPC-CW-NOA-RT can be viewed in **Table 9**.

**Table 9**: Ingredients added to SPC-CW-NOA-RT to make small scale batches A-G.

| Ingredients added to SPC-CW-NOA-RT (PHR) | A | B | C | D | E | F | G |
|---|---|---|---|---|---|---|---|
| Zinc Dimethacrylate | 2 | 0 | 2 | 3 | 2 | 3 | 2 |
| N-(1,3-dimethylbutyl)-N'-phenyl-p-phenylenediamine | 0 | 0 | 1 | 1 | 1 | 0.5 | 0.5 |
| Triallyl Isocyanurate | 0 | 2 | 0 | 0 | 1 | 0 | 1 |
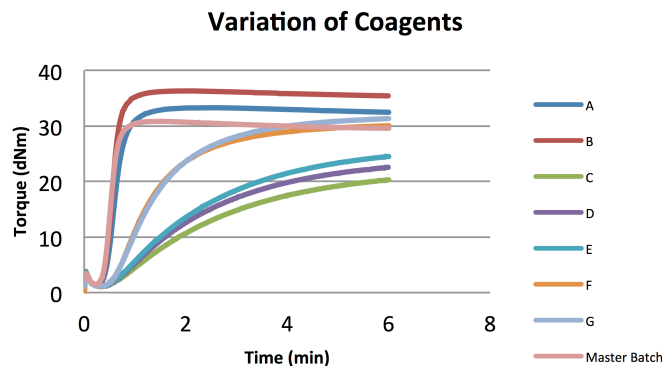
**Figure 36**: Variation of Coagents Rheological Profile.

By studying the rheological properties, it was determined that batch "F" was the most suitable to study adhesion because it has a slower cure rate than the master batch (as shown in the initial slope). However, it appeared that it could have similar physical properties to the master batch as evidenced by the final plateau regions of the curves. Batch "F" was adopted for larger scale production and became formulation SPC-CW-NOA+RT+ZDMA.

SPC-CW-NOA was produced as the result of using an older batch of SPC (approximately two months old) and finding out that the formulation yielded 100% rubber failure (5) when paired with SPS-L on cold-rolled steel. This observation was not seen previously and it was postulated that the non-polar process aids migrated out of the polar FKM during the two-month time span. Although this formulation did yield some rubber failure with all three adhesives (2) it was not the complete rubber failure that was previously seen.

The repeated lack of success caused the direction of the project to briefly change. At the time, it wasn't completely understood if the failure was due to RAF, CAF, or MAF. It was well known that bisphenol cured formulations adhered well to brass. It was decided that it could be possible to at least determine proper

pretreatment methods with the bisphenol cured system and eventually use the pretreatment methods with the peroxide cured system with steel. This yielded the bisphenol cured system (BPC). The ingredients used in the formulation are listed in **Table 10**.

Table 10: Ingredients in all Bisphenol Cured Formulations.

| Formulation | Bisphenol Cured (BPC) |
|---|---|
| Ingredient | PHR |
| Poly(vinylidenefluoride-co-hexafluoropropene)-1 | 80 |
| Poly(vinylidenefluoride-co-hexafluoropropene)-2 | 20 |
| Carbon Black | 25 |
| Treated Silica | 5 |
| Calcium Hydroxide | 3 |
| Magnesium Oxide | 15 |
| Carnauba Wax | 0.5 |
| Sulfolane | 0.5 |
| Benzyltriphenylphosphonium chloride | 1.8 |
| 4,4'-[2,2,2-Trifluoro-1-(trifluoromethyl)ethylidene] diphenol | 3 |

The rheological properties of all batches produced were studied. This proved to be very important when formulations with completely different curing mechanisms were utilized. **Figure 37** shows the rheological properties of BPC and that of SPC. The initial rheological behavior (approximately 30 seconds to 2 minutes) appears to be very different. The initial slope is believed to be an indicator of the rate of cure. **Figure 37** indicates that there is a much slower cure for the BPC versus SPC. The latter segments of the curves (approximately 2 minutes and later) also seem to vary by nearly 10 dNm, which, when compared to other curves, is a

significant difference. The rheological behavior observed as the curves level out

serve as a good indicator of the final mechanical properties of the cured rubber.
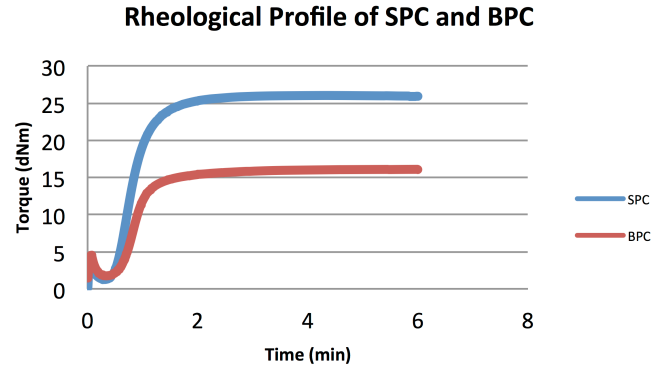


**Figure 37**: Rheological profile of the BPC compared to SPC.
As an attempt to obtain cohesive rubber failure the BPC was adhered to brass using UPSP-D and SPS-L.

**Figure 38** shows the adhesion data on BPC as well as SPC to brass. It is clear,

with all of the adhesives utilized, that the adhesion was far greater for the bisphenol

cured system than with the SPC. The large differences between the adhesion

effectiveness may be attributed, in part, to the difference in the curing mechanism.
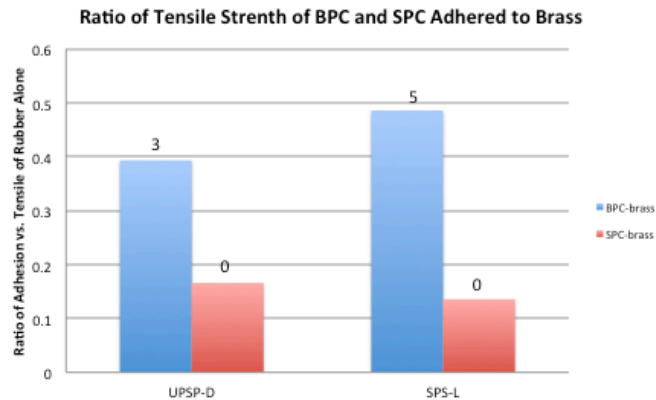


**Figure 38**: Adhesion studies of BPC and SPC.

After obtaining the BPC adhesion data to brass it made sense to determine

the effectiveness of the adhesion to steel. **Figure 39** shows the bonding

58

effectiveness of BPC adhered to both brass and steel. It was apparent that BPC was much better at bonding to steel than any of the SPC formulations.
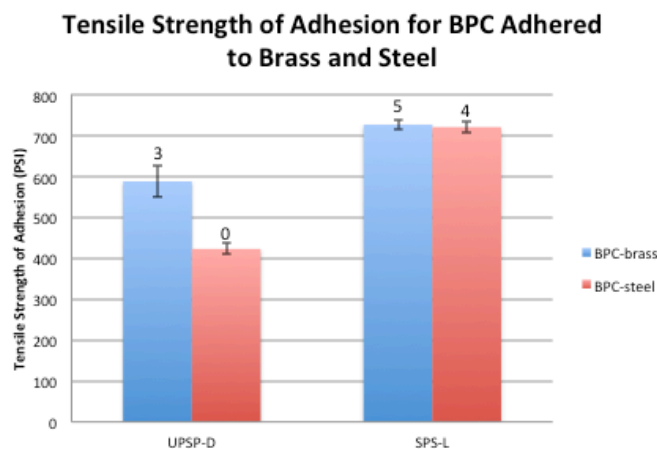


**Figure 39**: Tensile Strength of Adhesion for BPC Adhered to Brass and Steel.

It was hypothesized that the strong adhesion was, in part, due to the increased amount of base present in the BPC. This idea birthed the combi-cured systems (CC). The CC formulations are still characterized as being peroxide cured, however, it attempts to take advantage of some of the attributes of BPC systems as well. Formulation CC was made to be phenolic-like when discussing adhesion but is still peroxide cured. The TS was removed in the formulation as an attempt to use the polymeric silane in UPSP-D and UPS-L as a sensor to determine the locus of failure using ATR-FTIR. This formulation yielded a small amount of rubber failure and TS was added in formulation CC+TS in hopes to improve the rubber retention. **Table 11** shows the ingredients used in all CC formulations.

Table 11: Ingredients in all Combi-cured Formulations.

| Formulation | Combi-cured (CC) | CC+TS |
|---|---|---|
| Ingredient | PHR | PHR |
| PVTEM- 1 | 60 | |
| PVTEM - 2 | 40 | |
| Carbon Black (CB) | 5 | |
| Treated Silica (TS) | 0 | 10 |
| Calcium Hydroxide (CaOH) | 3 | |
| Magnesium Oxide (MgO) | 15 | |
| N-(1,3-dimethylbutyl)-N'-phenyl-p-phenylenediamine (RT) | 0.5 | |
| Zinc Dimethacrylate (ZDMA) | 3 | |
| Triallyl Isocyanurate (TAIC) | 3 | |
| 2,5-Dimethyl-2,5-di(t-butylperoxy)-hexane (DTBPH) | 2.5 | |

The adhesion effectiveness was determined for both the CC and CC+TS. The CC system did allow better adhesion than the average SPC, but much improvement was still needed. The addition of TS to the CC system caused larger changes in effects than was expected. The cure rate was significantly increased as evident in **Figure 40** and the final torque was much higher (~15 dNm) for CC+TS than it was for CC.
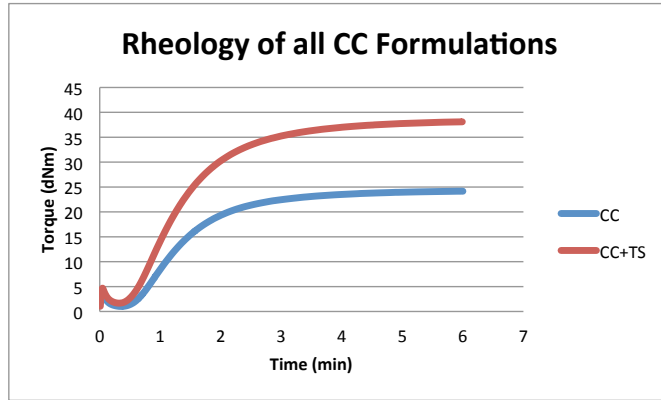
**Figure 40**: Rheology of all CC Formulations.

These changes were also noticed in the adhesion test when comparing the two CC systems, **Figure 41**. CC+TS consistently yielded high rubber failure (4-5). The variation between the samples within CC+TS was believed to be due to the differences in the cold rolled steel insert itself and not due to the rubber or adhesive. This led to many changes in the substrate preparation method and will be discussed in the Substrate and Substrate Preparation section.
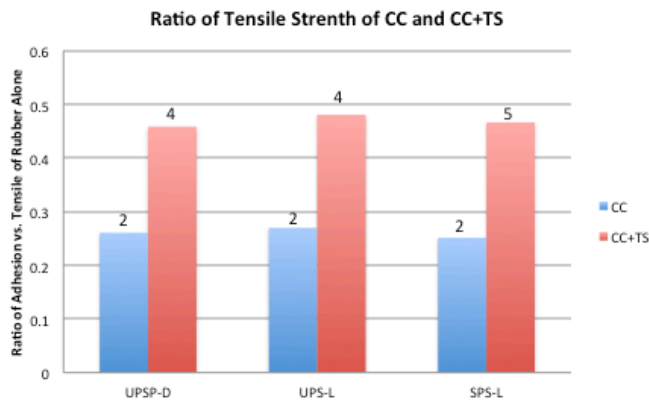


**Figure 41**: Ratio of Tensile Strength of CC and CC+TS.

The increased base used in the combi-cured systems seemed to be the key factor in obtaining the desired results. It is believed that the combi-cured systems

are still peroxide cured, but the increase in base allowed the adhesion to behave with some phenolic-like character.

### 3.2.3 Rubber Cure

It was hypothesized that a large amount of heat was lost while making the insert. To confirm this hypothesis, rheology was performed on the combi-cured system at 150°C for one hour to give an extended rheology curve, **Figure 42**.
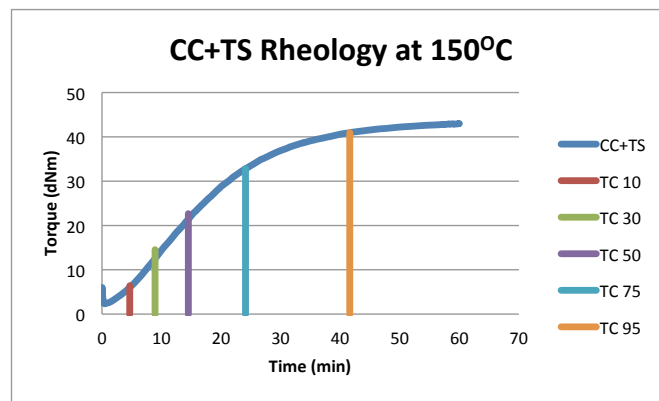


**Figure 42**: Extended rheology of CC at 150C. This data, along with **Equation 6**, was used to determine the conditions to obtain standard cures at 10%, 30%, 50%, 75%, and 95% of what is believed to be the final cure.

**Equation 6**: Equation to determine Torque at Theoretical Cure (TC).
$$(M_H - M_L) \times TC + M_L = \text{Torque at TC}$$

Using **Equation 6** and **Figure 42** the standard cure conditions were determined. Test slabs were all made at 150°C at the following times: 4 minutes 40 seconds, 8 minutes 55 seconds, 14 minutes 30 seconds, 24 minutes 6 seconds, and 41 minutes 36 seconds for theoretical cures of 10, 30, 50, 75 and 95%, respectively and immediately quenched with cold water.

AIs were also made in this way. **Figure 43** shows the ratio of the adhesion of the AI over the tensile of the rubber alone. This is an attempt to only view adhesion of the AI. When attempting to cure the part at TC 10 it was too under-cured to

62

properly make an AI. **Figure 43** does seem to confirm the hypothesis that extent of

cure is a major factor when determining the optimal adhesion.
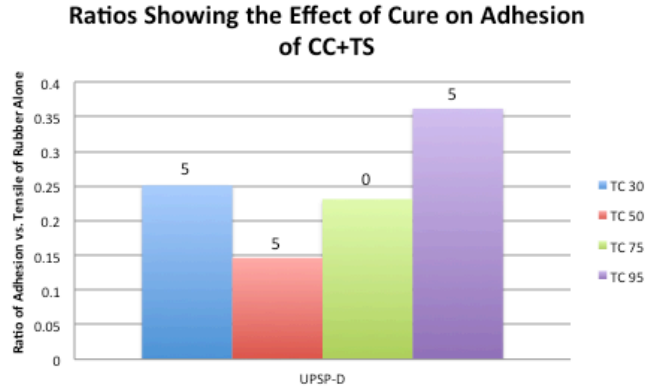


**Figure 43**: Adhesion of CC rubber to steel with UPSP-D. The temperature was held at 150°C and the cure time was varied to simulate different states of cure.

The amount of rubber retention varied from cure to cure. TC 30 and TC 50

consistently yielded 100% rubber failure, but the AI was extremely under cured so

very little stress was applied to the adhesive interfaces. TC 75 yielded failure at an

adhesive interface after a very large amount of elongation, which was indicative that

the AI was still under cured. TC 95 consistently yielded 100% cohesive rubber

failure (5) and did so while seeming to have an adequate cure to yield desirable

physical properties.

To determine the cure of previously made AIs, swell data were determined.

The same test slabs that we made for the standard cures were used for the swell

data, which were run in triplicate. Discs were cut out of the slabs and weighed

(Weight$_{initial}$) then placed in a solution of methyl ethyl ketone for three days at room

temperature and weighed again (Weight$_{swell}$). The discs were then allowed to dry at

room temperature for roughly 24 hours followed by heating in an oven at 100°C for

2 hours.  The discs were weighed for a final time (Weight$_{dry}$).  The % Swell was then

calculated using **Equation 7** and plotted vs. theoretical cure as seen in **Figure 44**.

**Equation 7**: Equation to determine %Swell.

$$\%\text{Swell} = \left( \frac{\text{Weight}_{swell} - \text{Weight}_{dry}}{\text{Weight}_{dry}} \right) \times 100$$
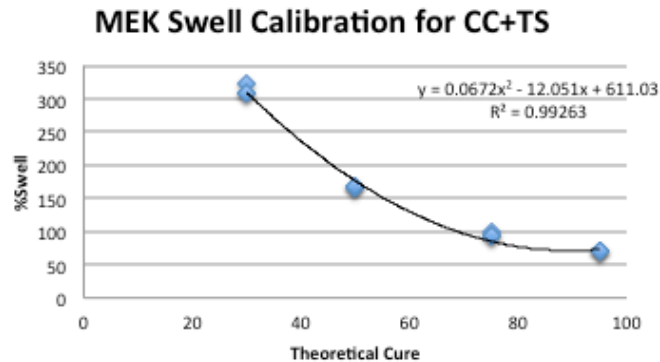


**Figure 44**: CC+TS swell data.

Although it was time consuming, the swell data proved to be an important

tool to determine the cure of the rubber.  Knowing that the modulus at 100%

elongation closely correlated to rubber cure, it was hypothesized that this

information could be also be used to determine the cure of the rubber as effectively

as swell data but take much less time.
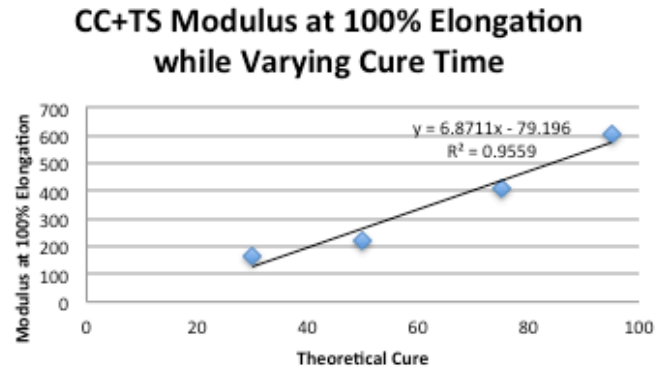
**Figure 45:** Calibration curve of modulus at 100% elongation vs. theoretical cure.

**Table 12: Different methods for determining cure.**

| AI | Cure of AI as determined by: | | %Difference |
| | Swell | 100% Modulus | |
|---|---|---|---|
| 1 | >95% | 116% | 20% |
| 2 | >95% | 98% | 3% |
| 3 | 52% | 48% | 8% |
| 4 | 62% | 60% | 4% |
| 5 | 71% | 79% | 11% |
| 6 | 76% | 89% | 15% |
| 7 | 72% | 78% | 8% |

To determine the validity of this method the cure, as determined by swell, was compared to cure as determined by modulus at 100% elongation using **Equation 8**. The results are displayed in Table 12.

**Equation 8:** %Difference equation for swell and Modulus at 100% Elongation.

$$\%\text{Difference} = \text{abs}\left(\frac{\text{Swell} - 100\%\ \text{Modulus}}{\text{average}(\text{Swell}, 100\%\text{Modulus})}\right) \times 100$$

Table 12 consists of a few unknown samples whose cure was determined by the known swell method and the Modulus at 100% Elongation Method. It should be noted that the swell could not be accurately calculated for AIs 1 and 2 because they

did not fall within the range of the calibration curve. Looking at the %Difference shows a reasonable agreement between the two methods. This shows that it is plausible that modulus at 100% elongation could be used instead of swell to determine the cure while concurrently reducing the time required from roughly one week (swell) to hours (modulus).

To determine the amount of heat that was lost due to the process the Apparent Cure of the AI was compared to what it should have been (Theoretical Cure). This was done by curing inserts using the theoretical cure conditions i.e. 150°C for the various times as shown in **Figure 42**. The residual disc, "the plug", was then subjected to the swell tests and the Apparent Cure was determined and compared to the theoretical cure, **Table 13**.

**Table 13:** Table Showing the Theoretical and Apparent Cures.

| Theoretical Cure | Apparent Cure | Difference |
|---|---|---|
| 30% | <10% | --- |
| 50% | <10% | --- |
| 75% | 41.45% | 33.55% |
| 95% | 66.37% | 28.63% |

The Apparent Cure could not be determined for the AIs cured to 30% and 50% because they did not fall within the calibration curve. When looking at the AIs cured at 75% and 95% it can be determined that roughly 30% of the Theoretical Cure was lost. This loss in the Apparent Cure can be attributed to the loss of heat due to the process.

## 3.3 Substrate and Substrate Preparation

Nearly all of the literature on adhesion stated that the most important factor to yield a good adhesive bond is the cleanliness of the substrate. That being considered the first test that was performed was to determine which pretreatment methods could yield acceptable adhesion. **Figure 46** shows the strength of adhesion (PSI) for various pretreatment methods to clean cold rolled steel along with the rubber retention (0-5) for SPC cured to UPSP-D. It was assumed that the pretreatment process would have a negligible effect on different adhesives.
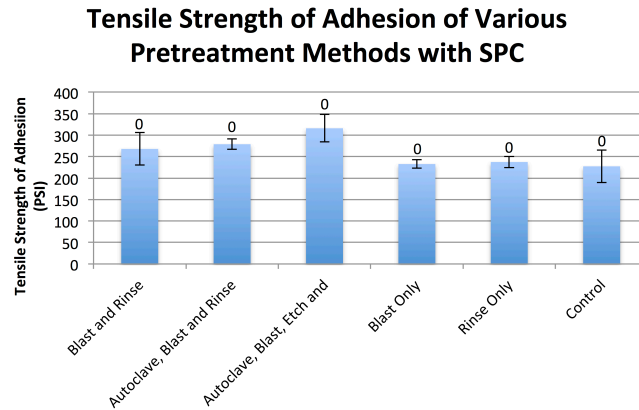


**Figure 46:** Adhesion of SPC to steel using UPSP-D along with rubber retention (0-5).

It was theorized that all of these methods could, individually, help adhesion but the combination that yielded maximum adhesion was not understood. At this point rubber retention was not a factor because all AIs had complete failure at the interface. Of the methods tested it appeared that the combination of using the autoclave followed by grit blasting and using a MEK solvent rinse yielded reasonable adhesion and was also quite reproducible. The method was believed to facilitate the formation of an oxide layer on the surface of the steel, which was then blasted with grit. The exposed layer underneath was believed to be good for chemical adhesion.

The chemical rinse was performed to remove machine oils used in making the part as well as water from the autoclave and any additional contaminants from the process.

The next factor studied was the application method for the adhesives. The two methods that were tested were dipping and spraying adhesive onto the metal insert. SPC was used for this test along with these adhesives: UPSP-D and SPS-L. The results are shown in **Figure 47**. Although the adhesion strength seemed to be greater for the dipped inserts with both adhesives, the increased reproducibility was desired from the sprayed inserts. Therefore the spray method was utilized throughout most of the project.
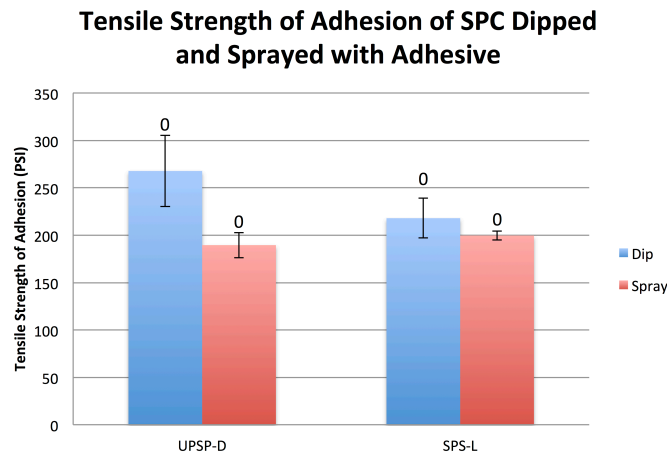


**Figure 47:** Adhesion of Dipping AI and spraying AIs.

## 3.4 DOE Experiments

Three sets of DOE experiments were used. All experiments consisted of 16 runs. MiniTab software was used to generate first order and second order relationships between the variables tested. These relationships were then used to make a regression. All combinations of variables were then used in the regression to determine the optimum formulation or pretreatment to use. The first, metal

pretreatment DOE, used steel inserts that were sprayed with UPSP-D.  The second

and third experiments (Formulation DOEs) used the optimum pretreatment method

found from the pretreatment DOE.  The Formulation DOEs were sprayed with either

UPS-L or SPS-L.  It was believed that since the likely curing mechanism was different

between the two adhesives the combination of ingredients needed to yield optimal

adhesion would be different as well.

### 3.4.1  Metal Pretreatment DOE

A metal pretreatment DOE was implemented to determine the effect specific

pretreatment steps had on adhesion: first solvent rinse, autoclave, grit blast, second

solvent rinse, and solvent flash on adhesion.  The DOE was designed to have five

variables, two levels (on or off), and 16 experiments.  The 16 experiments are

shown in **Table 6**.  The first solvent rinse (50:50 solution of methyl ethyl ketone and

toluene for 15 minutes) was added to remove all machine oils before the mechanical

and chemical pretreatments.  The autoclave was predicted to facilitate an oxide

layer, which could be removed by grit blasting the part.  The second solvent rinse

(50:50 solution of methyl ethyl ketone and toluene for 15 minutes) was added to

remove any contaminants that could have been gained from the previous steps.  The

solvent flash (3 minutes at $125^{o}C$) was implemented after the adhesive was sprayed

on the part and believed to keep the adhesive from flowing down the sides of the

part.

### 3.4.1.1    First Order Interactions

The main effects plot for rubber failure (**Figure 48**) shows some surprising results. It was anticipated that all steps of the pretreatment would, in fact, help adhesion. That the autoclave negatively impacted adhesion was very surprising. It was believed that the autoclave could have introduced a contaminant to the specimens resulting in the negative effect on adhesion. The grit blast was also expected to help adhesion. It was theorized that the grit blast would roughen the surface of the metal creating mechanical adhesion. The solvent rinses were expected to enhance adhesion but not to the extent of which they did. It appeared that the main contaminant on the steel was likely machine oils that were soluble in the rinse solution. The solvent flash was believed to help the adhesion as well. It was believed that the solvent had the ability to flow, but it appeared that adhesive flow was a non-factor for the rubber retention.
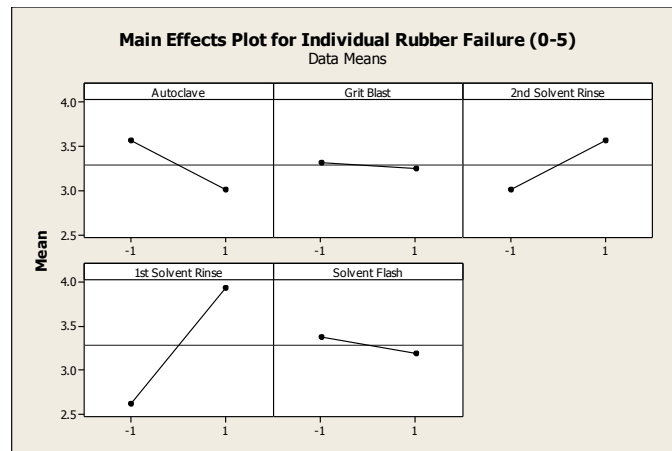


**Figure 48:** Main effects plot for Median Rubber Failure (0-5) for all pretreatment steps.

Not surprisingly, the adhesion strength (**Figure 49**) closely correlated to the rubber retention. The general direction (positive or negative slope) was the same

for all pretreatment steps with the exception of the grit blast. It is likely that the mechanical adhesion that was expected with rubber retention played a major role in the overall adhesion strength. The reasons for the negative effects seen with the autoclave and solvent flash for adhesion strength are likely the same as seen in rubber failure, with the same for the positive effects seen in the two solvent rinses.
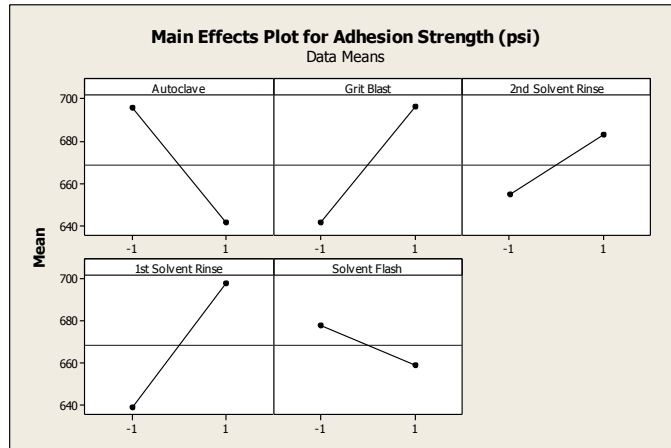


**Figure 49:** Main effects plot for adhesion strength (psi) for all pretreatment steps.

Surprisingly, although the autoclave seemed to interfere with adhesion strength it appeared that it helped make adhesion strength more repeatable, **Figure 50**. Just as surprising, the solvent flash increased the noise in the adhesion strength, which could be due to uneven heating in the heater. All the other steps decreased the noise in the system.
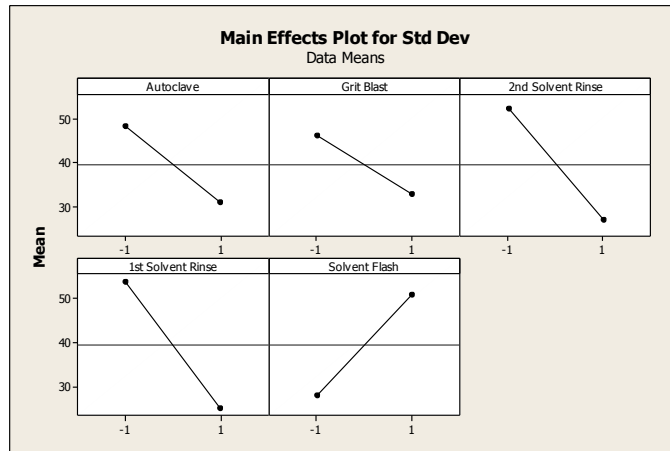
**Figure 50:** Main effects plot for standard deviation of adhesion strength (psi) for all pretreatment steps.

### 3.4.1.2    Second Order Interactions

After determining the effect sole pretreatment steps had on the variable pretreatment steps it was necessary to determine the effect of the interactions between the pretreatment steps.  When viewing the interaction plots for rubber failure (**Figure 51**) it can be seen that many of the pretreatment steps worked together to yield negative results.  For instance, the plot shows that when a pretreatment method uses both the autoclave and the second solvent rinse, the solvent rinse will be less effective than if the solvent rinse was used by itself.  This is likely due to the conditions of the autoclave making contaminants on the insert more difficult to remove.
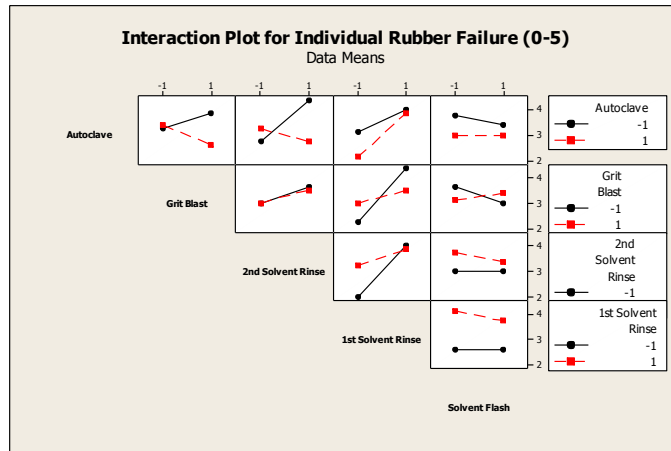
**Figure 51:** Interaction plot for the individual rubber failure for the pretreatment steps utilized.

After studying individual rubber failure, the way the interactions affected adhesion strength was studied, **Figure 52**. Again very few interactions yielded positive interactions. Most of the interactions seemed to negate each other including autoclave-grit blast, grit blast-solvent flash, and 1st solvent rinse-solvent flash. It was expected that there would be more positive interactions for both of these plots (**Figure 51** and **Figure 52**). These plots show that the anticipated positive interaction between the autoclave and grit blast does not exist.
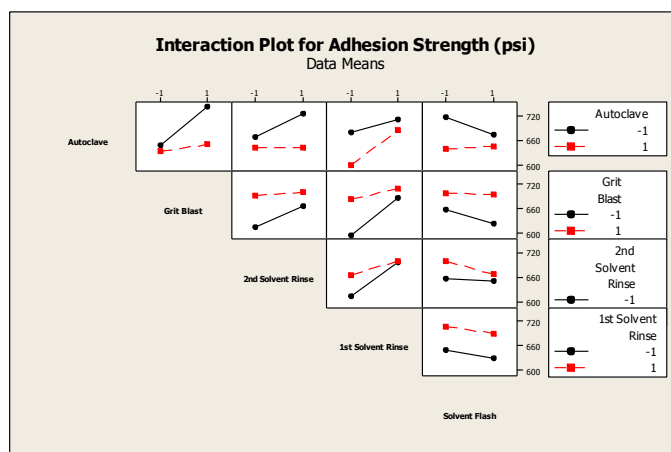


**Figure 52:** Interaction plot for the adhesion strength (psi) for the pretreatment steps utilized.

73

Once again the interaction effect on standard deviation of the adhesion strength was studied, **Figure 53**. These plots show that standard deviation is greatly affected by the second order interactions. The majority of the plots show positive interactions between two pretreatment steps yielding less noise in the adhesion strength including: the second solvent rinse-solvent flash, and the grit blast with the solvent flash.
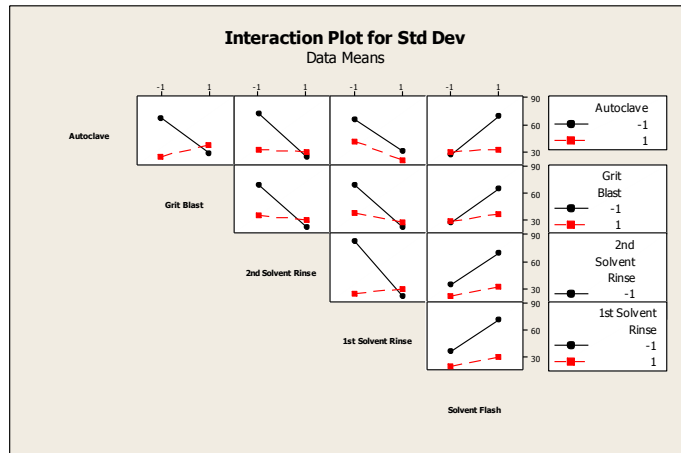


**Figure 53:** Interaction plot for the standard deviation of the adhesion strength (psi) for the pretreatment steps utilized.

### 3.4.1.3 Regression

The first and second order interactions were analyzed using a stepwise regression to determine which interactions were significant to the variable. **Table 14** shows the coefficients for median rubber failure as well as median tensile at cursor for the pretreatment steps. A regression was not made for standard deviation of adhesion strength because it was a less important factor than median rubber failure and adhesion strength.

**Table 14:** Coefficients for Rubber Failure and Adhesion Strength for Pretreatment Steps.

| Rubber Failure | | Adhesion Strength | |
|---|---|---|---|
| Term | Coefficient | Term | Coefficient |
| Constant | 3.28 | Constant | 677.82 |
| Autoclave | -0.28 | Autoclave | -36.55 |
| Grit Blast | -0.03 | Grit Blast | 18.69 |
| 2nd Solvent Rinse | 0.28 | 2nd Solvent Rinse | 5.33 |
| 1st Solvent Rinse | 0.66 | 1st Solvent Rinse | 20.54 |
| Solvent Flash | -0.09 | Autoclave x 2nd Solvent Rinse | -5.55 |
| Autoclave x 2nd Solvent Rinse | -0.53 | Grit Blast x 1st Solvent Rinse | -7.28 |
| Grit Blast x 1st Solvent Rinse | -0.41 | 2nd Solvent Rinse x 1st Solvent Rinse | -3.73 |
| 2nd Solvent Rinse x1st Solvent Rinse | -0.34 | Autoclave x Grit Blast | -10.62 |
| Autoclave x Gritblast | -0.34 | Autoclave x 1st Solvent Rinse | 22.28 |
| Grit Blast x Solvent Flash | 0.22 | 2nd Solvent Rinse x Solvent Flash | -15.98 |
| Autoclave x First Solvent Rinse | 0.22 | 1st Solvent rinse x Solvent Flash | -7.49 |
| --- | --- | Autoclave x Solvent Flash | 4.02 |

It appeared that when considering both rubber failure and adhesion strength, the autoclave played the biggest role. Surprisingly, this role was negative. The grit blast had a negative effect on the rubber failure but actually had a positive role on the adhesion strength. The first solvent rinse was the greatest positive influence on both the adhesion strength and rubber failure indicating that a clean surface is necessary for good adhesion.

The coefficients were then used to determine the optimal combination of pretreatment steps by calculating all 32 possible combinations and determining their effect on adhesion and rubber failure as seen in **Table 15**. It was determined that the two solvent rinses were the only two pretreatment steps needed to yield maximum rubber retention and nearly maximum adhesion strength. It was decided that this combination would be better because the combination of ingredients that yielded highest adhesion strength contained steps that may not be suitable for substrates besides steel. The errors associated with the predicted adhesion strength and rubber failure were considered to be reasonable but not great for the pretreatment steps.

**Table 15:** Chart showing predicted and actual (if applicable) rubber failure and adhesion strength (psi) for all pretreatment combinations.

| DOE Number | 1st Solvent Rinse | Autoclave | Grit Blast | 2nd Solvent Rinse | Solvent Flash | Adhesion Strength, Predicted (PSI) | Adhesion Strength, Actual (PSI) | % Error | Rubber Failure, Predicted (PSI) | Rubber Failure, Actual (PSI) | % Error |
|---|---|---|---|---|---|---|---|---|---|---|---|
| 1 | -1 | -1 | 1 | 1 | 1 | 754.8 | 751.4 | 0.5% | 4.3 | 5 | -15.1% |
| 2 | -1 | -1 | -1 | 1 | -1 | 706.7 | 706.7 | 0.0% | 3.0 | 4 | -28.6% |
| 3 | 1 | 1 | 1 | 1 | 1 | 661.5 | 658.1 | 0.5% | 1.8 | 3 | -50.0% |
| 4 | -1 | -1 | -1 | -1 | 1 | 684.4 | 539.2 | 23.7% | 0.5 | 2 | -120.0% |
| 5 | 1 | -1 | 1 | -1 | 1 | 637.8 | 731.1 | -13.6% | 2.6 | 4 | -42.4% |
| 6 | 1 | 1 | -1 | 1 | -1 | 698.8 | 698.9 | 0.0% | 3.5 | 5 | -35.3% |
| 7 | 1 | -1 | -1 | -1 | -1 | 552.1 | 676.5 | -20.2% | 2.7 | 4 | -38.8% |
| 8 | 1 | 1 | -1 | -1 | 1 | 699.8 | 699.7 | 0.0% | 4.5 | 5 | -10.5% |
| 9 | 1 | -1 | -1 | 1 | 1 | 582.2 | 672.8 | -14.4% | 2.7 | 4 | -38.8% |
| 10 | -1 | 1 | 1 | -1 | 1 | 732.0 | 636.9 | 13.9% | 4.0 | 2 | 66.7% |
| 11 | 1 | 1 | -1 | -1 | -1 | 676.3 | 679.8 | -0.5% | 3.2 | 4 | -22.2% |
| 12 | -1 | 1 | 1 | 1 | 1 | 670.2 | 584.7 | 13.6% | 4.1 | 2 | 68.9% |
| 13 | 1 | -1 | 1 | 1 | -1 | 621.8 | 770.2 | -21.3% | 3.0 | 5 | -50.0% |
| 14 | -1 | 1 | -1 | 1 | -1 | 769.3 | 622.6 | 21.1% | 4.1 | 2 | 68.9% |
| 15 | -1 | -1 | 1 | -1 | -1 | 679.0 | 549.6 | 21.1% | 4.3 | 2 | 73.0% |
| 16 | -1 | -1 | 1 | -1 | -1 | 718.6 | 722.1 | -0.5% | 2.2 | 3 | -30.8% |
| | -1 | -1 | -1 | -1 | -1 | 645.5 | | | 0.7 | | |
| | -1 | -1 | -1 | 1 | 1 | 681.6 | | | 2.8 | | |
| | -1 | -1 | 1 | -1 | 1 | 757.5 | | | 2.0 | | |
| | -1 | -1 | 1 | 1 | -1 | 779.8 | | | 4.5 | | |
| | -1 | 1 | -1 | -1 | 1 | 687.9 | | | 4.2 | | |
| | -1 | 1 | -1 | 1 | -1 | 725.2 | | | 5.3 | | |
| | -1 | 1 | 1 | -1 | -1 | 723.1 | | | 4.2 | | |
| | -1 | 1 | 1 | 1 | 1 | 714.3 | | | 4.9 | | |
| | 1 | -1 | -1 | -1 | -1 | 607.1 | | | 2.5 | | |
| | 1 | -1 | -1 | 1 | -1 | 591.1 | | | 2.9 | | |
| | 1 | -1 | 1 | -1 | -1 | 582.8 | | | 2.8 | | |
| | 1 | -1 | 1 | 1 | 1 | 612.8 | | | 2.8 | | |
| | 1 | 1 | -1 | -1 | 1 | 674.7 | | | 4.7 | | |
| | 1 | 1 | -1 | 1 | 1 | 659.9 | | | 3.3 | | |
| | 1 | 1 | 1 | -1 | 1 | 701.3 | | | 3.0 | | |
| | 1 | 1 | 1 | 1 | -1 | 700.4 | | | 2.0 | | |

### 3.4.1.4    IR Confirmation

These data were confirmed using ATR FT-IR.  A spectrum of an insert, as received, was obtained (**Figure 54**).  The spectrum of the same insert was obtained after each major step of the pretreatment.  The only noticeable difference in the

spectrum is the disappearance of the peaks around 2853 cm$^{-1}$ and 2922 cm$^{-1}$ after the first solvent rinse that were originally seen on the insert, as received.
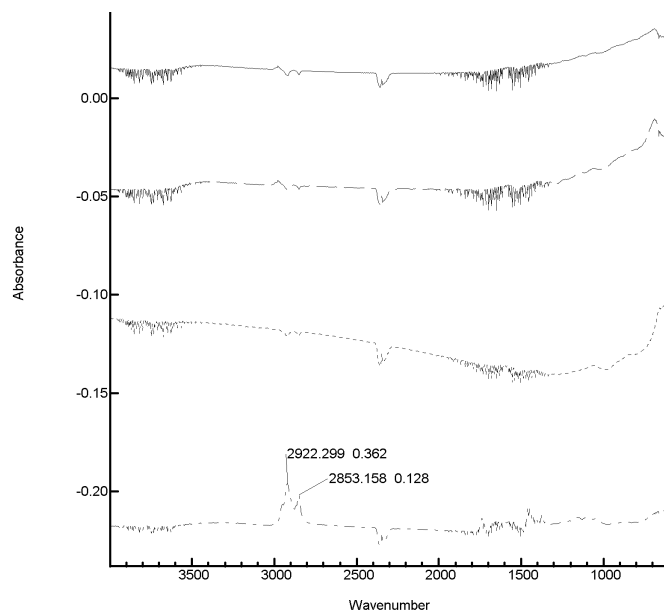


**Figure 54:** IR data of a steel insert as received and after each pretreatment step.

## 3.4.2  Rubber Formulation DOE

A formulation DOE was implemented to determine the effect specific ingredients had on adhesion: CB, TS (**Figure 55a**), NOA (**Figure 55b**), and ZDMA (**Figure 55c**), and CW (**Figure 55d**) on two separate adhesives: UPS-L and SPS-L. The DOE was designed to have five variables, two levels (on or off), and 16 experiments.  The 16 experiments are shown in **Table 7**.
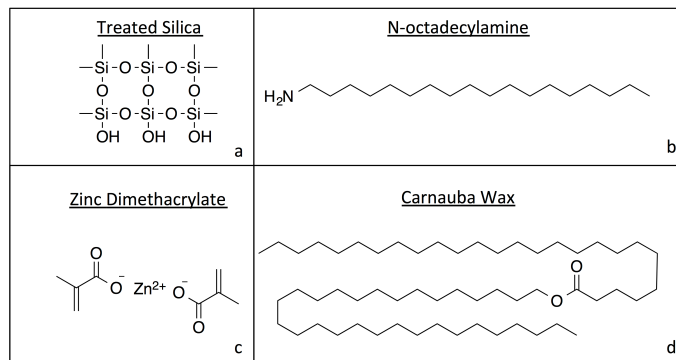
**Figure 55**: Structures of ingredients studied in formulation DOE.

## 3.4.2.1 First order Interactions

The effect on adhesion (0-5) and adhesion tensile strength (psi), the standard deviation of the tensile strength of all first order interactions were studied. This was viewed by looking at the difference of the main effects between the adhesion (0-5), adhesion tensile strength (psi), the standard deviation of the tensile strength, when the specific ingredient was and was not used.

**Figure 56** shows the main effects on median rubber failure by comparing the average of the values when the specific ingredient is and is not used. The plots on the left are for the unsaturated polymeric silane (UPS-L). These plots, along with the plots on the right (SPS-L), show that carbon black, treated silica, and carnauba wax have a positive impact on the rubber retention whereas *N*-octadecylamine and zinc dimethacrylate have negative effects. The positive effects for carbon black and treated silica were expected. Carbon black is the most widely used reinforcing filler used in rubber and is known to enhance adhesion by non-chemically interacting with the elastomer. [53] The more noticeable rubber retention for SPS-L was not expected. It was believed that since the carbon black aids by non-chemical interactions that the increase would be similar. The treated silica was believed to

78

cause the greatest increase in rubber retention by possibly adhering to the steel as well as the surface of the steel through the silanol functional groups present, **Figure 55a**. This increase in rubber retention was seen with both UPS-L and SPS-L. Carnauba wax was expected to decrease the rubber retention because its role as a process aid and its hydrophobic nature, but the increase in rubber retention was so slight that it was considered insignificant.
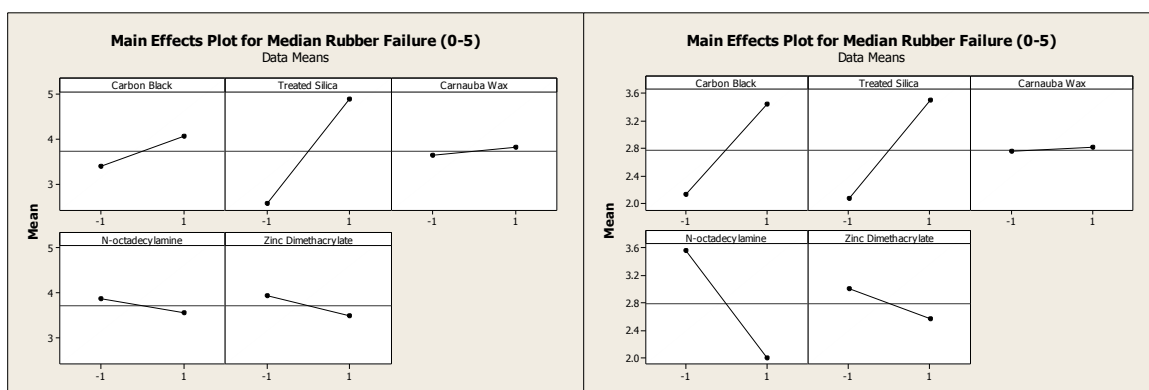


**Figure 56:** Main effects plot for Median Rubber Failure for UPS-L (left) and SPS-L (right).

Unexpectedly, zinc dimethacrylate and *N*-octadecylamine had a negative effect on the rubber retention with both adhesives. The unique structure of zinc dimethacrylate, **Figure 55c,** has been shown to increase rubber retention by Henning et. al. [52] Zinc dimethacrylate has the ability to crosslink through the polymer as well as bond to the metal substrate.

When protonated at the amine nitrogen, *N*-octadecylamine (**Figure 55b**) falls into a category known as surfactants due to its hydrophilic head and hydrophobic tail. This structure allows the process aid to migrate to the surface of the polar FKM allowing the rubber to be easily removed from the mixer. Due to this phenomenon, the *N*-octadecylamine was expected to have a negative effect on adhesion. The *N*-

octadecylamine proved to have a negative effect on both adhesives, but the effect was much greater for SPS-L. A possibility for the greater interference is that the *N*-octadecylamine could possibly react with the SPS-L by proton exchange.

Main effect plots for Adhesion Strength (psi) were also studied (**Figure 57**). The adhesion strength generally has a positive correlation, which was to be expected. The only noticeable exception is for the zinc dimethacrylate of both adhesives. In the case of adhesion strength the zinc dimethacrylate behaved as expected by increasing the adhesion strength. This increase is believed to be due to the ZDMA adhering well to both the rubber through the alkene and the steel.
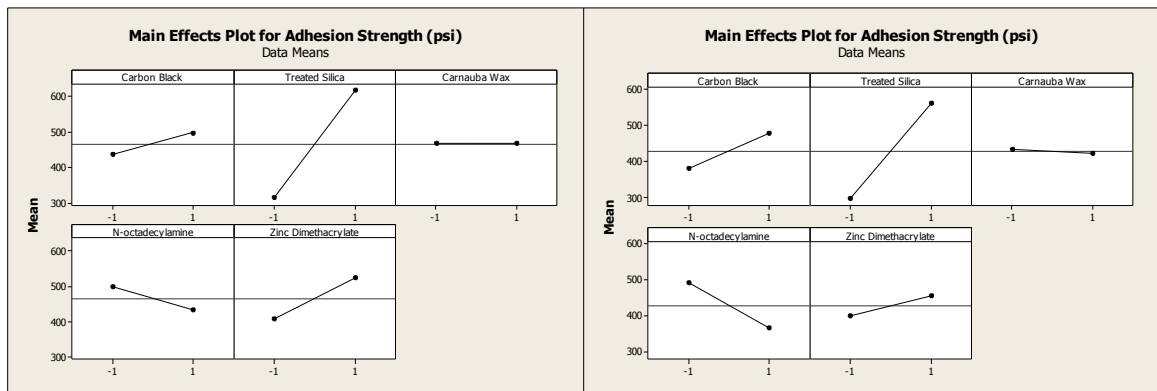


**Figure 57:** Main effects plots for Adhesion Strength (psi) for UPS-L (l) and SPS-L (r).

The standard deviation main effects were also studied and, with the rubber retention and adhesion strength, a maximum value was preferred. This is not the case with the standard deviation. An increase in these plots represents noise added to the system. The main effects for standard deviation show little similarities when comparing adhesives. One aspect that needs to be considered when comparing the standard deviations is that mixed rubber does not reach homogeneity. This in itself can add noise to the system.

All standard deviations in both plots are miniscule enough when compared to the adhesion strength that they do not appear significant (ie. the adhesion strength for samples that contained *N*-octadecylamine were ~375 psi and the standard deviation was ~45 psi, roughly 12%, which is typically considered acceptable in the rubber industry).
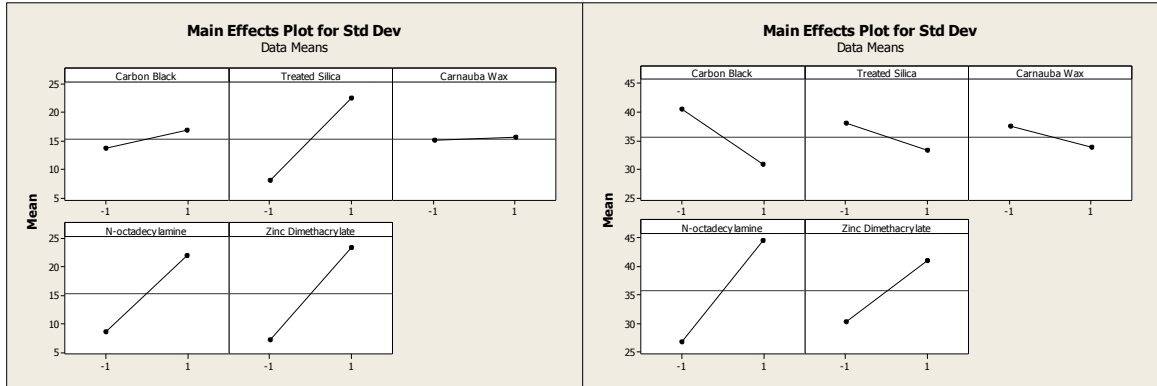


**Figure 58:** Main effects plots for standard deviation of Adhesion Strength (psi) for UPS-L (l) and SPS-L (r).

### 3.4.2.2 Second Order Interactions

Second order plots were also generated to study the effects two specific ingredients had on the variables studied. The interaction plots look at the mean of four sets of data: both ingredients being used, both ingredients not being used, and each ingredient being used separately. The first set of interaction plots, **Figure 59**, studied the median rubber failure for rubber cured with UPS-L (left) and SPS-L (right). Overall there are not a lot of interactions between the different ingredients. The interaction between carbon black and treated silica seems to be positive but the silica was unaffected by the presence of carbon black when cured to UPS-L. This was to be expected because silica was expected to chemically help adhesion whereas carbon black was only expected to help physically. When looking at SPS-L,

81

using both carbon black and treated silica seems to help rubber failure. One of the more interesting interactions is between *N*-octadecylamine and zinc dimethacrylate bonded to SPS-L. This showed that when both ingredients were used they inhibited rubber failure more than either of the ingredients acting alone.
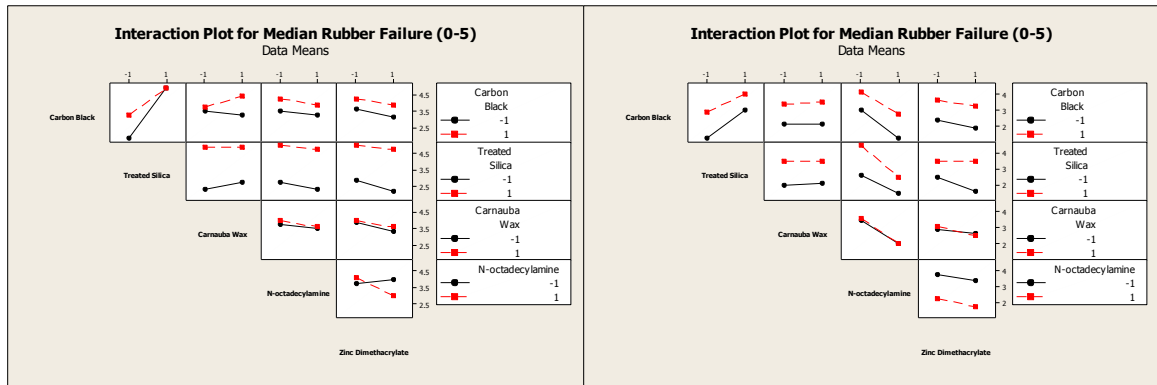


**Figure 59:** Interaction plot for median rubber failure (0-5) with UPS-L (left) and SPS-L (right).

The way second order interactions affected adhesion strength was also studied as shown in **Figure 60**. Again the second order interactions of the adhesion strength correlated closely to the second order reactions of median rubber failure. Treated silica and ZDMA seemed to have the greatest interaction increase for UPS-L. The carnauba wax seemed to have no effect on ZDMA because the values are roughly the same whether carnauba wax is used or not.
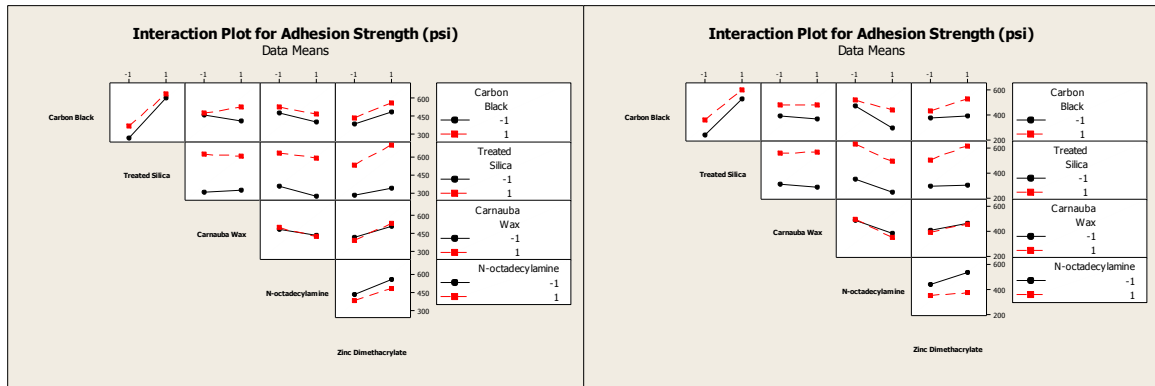
**Figure 60:** Interaction plot for adhesion strength with UPS-L (l) and SPS-L (r).

The interaction plot for standard deviation, **Figure 61**, showed a lot of variation. For instance, including both ZDMA and treated silica greatly increases the noise in adhesion strength for both adhesives. One of the more interesting interactions is when *N*-octadecylamine is cured with and without carbon black. When *N*-octadecylamine is cured without carbon black the noise is much higher than when it is cured with carbon black.
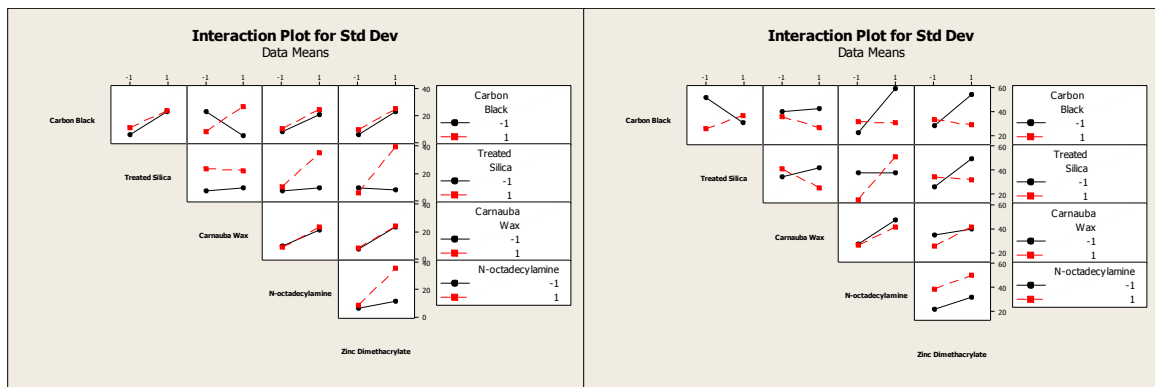


**Figure 61:** Interaction plot for standard deviation of the adhesion strength with UPS-L (l) and SPS-L (r).

### 3.4.2.3 Regression

The first and second order interactions were analyzed using a stepwise regression to determine which interactions were significant to the variable. **Table 16** shows the coefficients for median rubber failure as well as median tensile at

83

cursor for UPS-L. A regression was not made for standard deviation of adhesion strength because it was a less important factor than median rubber failure and adhesion strength.

**Table 16:** Coefficients for Rubber Failure and Adhesion Strength for UPS-L.

| Median Rubber Failure | | Adhesion Strength | |
|---|---|---|---|
| **Term** | **Coefficients** | **Term** | **Coefficients** |
| Constant | 3.71875 | Constant | 465.841 |
| Treated Silica | 1.15625 | Treated Silica | 151.954 |
| Carbon Black | 0.34375 | Zinc Dimethacrylate | 57.044 |
| Carbon Black x Treated Silica | -0.34375 | N-octadecylamine | -31.489 |
| N-octadecylamine x Zinc Dimethacrylate | -0.34375 | Carbon Black | 30.931 |
| Zinc Dimethacrylate | -0.21875 | Treated Silica x Zinc Dimethacrylate | 26.904 |
| Carbon Black x Carnauba Wax | 0.21875 | Carbon Black x Carnauba Wax | 25.289 |
| N-octadecylamine | -0.15625 | Carbon Black x Treated Silica | -17.006 |
| Carnauba Wax | 0.09375 | Treated Silica x N-octadecylamine | 10.469 |
| Treated Silica x Carnauba Wax | -0.09375 | Carbon Black x Zinc Dimethacrylate | 4.696 |
| Treated Silica x Zinc Dimethacrylate | 0.09375 | --- | --- |

The terms are ordered by their significance to the effect. The larger the magnitude of the coefficient the greater the effect it has on the variable. Treated silica is the most significant variable to both the median rubber failure and adhesion strength. The sign of the first order variables i.e. Carnauba wax, treated silica, carbon black shows whether it helps (positive value) or hurts (negative value) the variable studied. In regards to the coefficients of the second order interactions, i.e. Carbon Black x Treated Silica, Carbon Black x Carnauba Wax, and Treated Silica x *N*-octadecylamine, if the coefficient is positive, then both ingredients have to be in sync for a positive effect to occur. The effect will be positive whether both ingredients are on or off. The effect will be negative when only one of the two variables is used

in the rubber formulation.  These effects flip when the coefficient for a second order

reaction is negative.

**Table 17:** Coefficients for Rubber Failure and Adhesion Strength for SPS-L.

| Median Rubber Failure | | Adhesion Strength | |
|---|---|---|---|
| **Term** | **Coefficients** | **Term** | **Coefficients** |
| Constant | 2.78125 | Constant | 427.228 |
| N-octadecylamine | -0.78125 | Treated Silica | 133.257 |
| Treated Silica | 0.71875 | N-octadecylamine | -63.154 |
| Carbon Black | 0.65625 | Carbon Black | 49.424 |
| Zinc Dimethacrylate | -0.21875 | Zinc Dimethacrylate | 28.566 |
| Treated Silica x N-octadecylamine | -0.21875 | Treated Silica x Zinc Dimethacrylate | 27.326 |
| Treated Silica x Zinc Dimethacrylate | 0.21875 | Carbon Black x N-octadecylamine | 26.2 |
| Carbon Black x Treated Silica | -0.15625 | Carbon Black x Zinc Dimethacrylate | 20.092 |
| Carbon Black x N-octadecylamine | 0.09375 | N-octadecylamine x Zinc Dimethacrylate | -19.54 |
| CarnaubaWax x Zinc Dimethacrylate | -0.09375 | --- | --- |

The coefficients for median rubber failure and adhesion strength for SPS-L

are shown in **Table 17**.  Unlike the coefficients found for UPS-L, the most significant

factor for rubber retention was the inhibition of *N*-octadecylamine.  This is believed

to react with the adhesive, likely a proton exchange mechanism, which can inhibit

the rubber retention.   Treated silica was still a major factor and contributed

positively to both the adhesion strength and median rubber failure.

The terms were given a value of 1 if it was used and -1 if it was not used.  If

the term was a first order term then the value was multiplied by the coefficient.  If

the term was a second order term then the product of both values were found and

then multiplied by the coefficient.  The sum of all of the products and the constant

was the predicted rubber failure.  **Equation 9** shows an example calculation of how

the predicted rubber failure is determined for a single run with SPS-L adhesive.  The

10<sup>th</sup> run used CB, TS and ZDMA and did not use Carnauba wax and *N*-octadecylamine.

**Equation 9:** Example Calculation of Predicted Rubber Failure for 10<sup>th</sup> Run with SPS-L Adhesive.

$$= \text{constant} + (1.15625 \times TS) + (0.34375 \times CB) - (0.34375 \times CB \times TS)$$
$$- (0.34375 \times NOA \times ZDMA) - (0.21875 \times ZDMA) + (0.21875 \times CB \times CW)$$
$$- (0.15625 \times NOA) + (0.09375 \times CW) - (0.09375 \times TS \times CW)$$
$$+ (0.09375 \times TS \times ZDMA)$$
$$= 3.71875 + (1.15625 \times 1) + (0.34375 \times 1) - (0.34375 \times 1 \times 1) - (0.34375 \times -1 \times 1)$$
$$- (0.21875 \times 1) + (0.21875 \times 1 \times -1) - (0.15625 \times -1)$$
$$+ (0.09375 \times -1) - (0.09375 \times 1 \times -1) + (0.09375 \times 1 \times 1)$$
$$= 5$$

The predicted rubber failure and adhesion strength was calculated for each of the 32 possible combinations of ingredients for both adhesives. **Table 18** contains the ingredients used, the predicted median rubber failure, and the predicted median adhesion strength for UPS-L.  The maximum rubber retention and adhesion strength was obtained using the same combination of ingredients: carbon black, treated silica, carnauba wax, and zinc dimethacrylate.   This specific combination omitted *N*-octadecylamine.  The maximum rubber retention was about 5.5 and the adhesion strength was about 767 psi.

**Table 18**: Chart showing predicted and actual (if applicable) rubber failure and adhesion strength (psi) for all rubber ingredient combinations adhered with UPS-L.

| DOE Number | Carbon Black | Treated Silica | Carnauba Wax | N-octadecylamine | Zinc Dimethacrylate | Adhesion Strength, Predicted (PSI) | Adhesion Strength, Actual (PSI) | % Error | Rubber Failure, Predicted | Rubber Failure, Actual | % Error |
|---|---|---|---|---|---|---|---|---|---|---|---|
| 1 | -1 | 1 | 1 | -1 | 1 | 678.9 | 701.2 | -3.2% | 5.0 | 5 | 0.0% |
| 2 | -1 | -1 | 1 | -1 | -1 | 257.2 | 256.0 | 0.5% | 2.0 | 2 | 0.0% |
| 3 | 1 | 1 | 1 | 1 | 1 | 724.6 | 726.0 | -0.2% | 4.5 | 4 | 11.8% |
| 4 | -1 | -1 | -1 | 1 | 1 | 358.6 | 346.1 | 3.5% | 2.1 | 2 | 4.9% |
| 5 | -1 | 1 | -1 | 1 | 1 | 687.4 | 675.1 | 1.8% | 4.5 | 4 | 11.8% |
| 6 | 1 | 1 | 1 | 1 | -1 | 310.3 | 309.9 | 0.1% | 4.2 | 4 | 4.9% |
| 7 | -1 | -1 | -1 | 1 | -1 | 223.8 | 235.1 | -4.9% | 2.4 | 3 | -22.2% |
| 8 | 1 | -1 | -1 | 1 | 1 | 329.4 | 316.1 | 4.1% | 2.0 | 2 | 0.0% |
| 9 | -1 | -1 | 1 | 1 | 1 | 224.1 | 226.6 | -1.1% | 1.0 | 1 | 0.0% |
| 10 | 1 | 1 | -1 | 1 | 1 | 716.1 | 704.7 | 1.6% | 5.0 | 5 | 0.0% |
| 11 | 1 | -1 | -1 | 1 | -1 | 496.8 | 531.2 | -6.7% | 5.0 | 5 | 0.0% |
| 12 | 1 | -1 | 1 | -1 | 1 | 463.9 | 487.3 | -4.9% | 3.8 | 4 | -5.1% |
| 13 | -1 | 1 | 1 | 1 | -1 | 478.3 | 454.7 | 5.1% | 5.0 | 5 | 0.0% |
| 14 | 1 | 1 | 1 | -1 | -1 | 589.4 | 565.0 | 4.2% | 5.0 | 5 | 0.0% |
| 15 | 1 | 1 | -1 | -1 | -1 | 343.7 | 334.0 | 2.9% | 3.0 | 4 | -28.6% |
| 16 | -1 | 1 | -1 | -1 | -1 | 570.9 | 584.5 | -2.3% | 5.0 | 5 | 0.0% |
|  | -1 | -1 | -1 | -1 | -1 | 307.8 |  |  | 2.0 |  |  |
|  | -1 | -1 | -1 | 1 | 1 | 274.7 |  |  | 1.1 |  |  |
|  | -1 | -1 | 1 | -1 | 1 | 308.1 |  |  | 2.0 |  |  |
|  | -1 | -1 | 1 | 1 | -1 | 173.3 |  |  | 2.3 |  |  |
|  | -1 | 1 | -1 | -1 | 1 | 729.4 |  |  | 5.5 |  |  |
|  | -1 | 1 | -1 | 1 | -1 | 528.9 |  |  | 5.4 |  |  |
|  | -1 | 1 | 1 | -1 | -1 | 520.3 |  |  | 4.6 |  |  |
|  | -1 | 1 | 1 | 1 | 1 | 636.8 |  |  | 4.0 |  |  |
|  | 1 | -1 | -1 | -1 | 1 | 413.3 |  |  | 3.0 |  |  |
|  | 1 | -1 | -1 | 1 | -1 | 259.7 |  |  | 3.3 |  |  |
|  | 1 | -1 | 1 | -1 | -1 | 394.2 |  |  | 3.8 |  |  |
|  | 1 | -1 | 1 | 1 | 1 | 380.0 |  |  | 2.8 |  |  |
|  | 1 | 1 | -1 | -1 | -1 | 538.8 |  |  | 4.6 |  |  |
|  | 1 | 1 | -1 | 1 | 1 | 674.1 |  |  | 4.0 |  |  |
|  | 1 | 1 | 1 | -1 | 1 | 766.7 |  |  | 5.5 |  |  |
|  | 1 | 1 | 1 | 1 | -1 | 547.3 |  |  | 5.4 |  |  |

**Table 19** contains the ingredients used, the predicted median rubber failure, and the predicted median adhesion strength for all possible 32 ingredient combinations cured with SPS-L. The highest adhesion strength as well as maximum rubber retention came from the combination of using carbon black, treated silica, and zinc dimethacrylate making it the best combination for bonding to SPS-L. This

87

particular combination omitted both process aids: CW and NOA, although adding

CW does not drastically affect the adhesion.

**Table 19:** Chart showing predicted and actual (if applicable) rubber failure and adhesion strength (psi) for all rubber ingredient combinations adhered with SPS-L.

| DOE Number | Carbon Black | Treated Silica | Carnauba Wax | N-octadecylamine | Zinc Dimethacrylate | Adhesion Strength, Predicted (PSI) | Adhesion Strength, Actual (PSI) | % Error | Rubber Failure, Predicted | Rubber Failure, Actual | % Error |
|---|---|---|---|---|---|---|---|---|---|---|---|
| 1 | -1 | 1 | 1 | -1 | 1 | 694.9 | 683.3 | -1.7% | 4.0 | 4 | 0.0% |
| 2 | -1 | -1 | 1 | -1 | -1 | 334.2 | 298.8 | -10.6% | 2.4 | 3 | 23.1% |
| 3 | 1 | 1 | 1 | 1 | 1 | 630.4 | 613.5 | -2.7% | 3.0 | 3 | 0.0% |
| 4 | -1 | -1 | -1 | -1 | 1 | 373.8 | 326.8 | -12.6% | 1.6 | 2 | 28.0% |
| 5 | -1 | 1 | -1 | 1 | 1 | 477.2 | 452.9 | -5.1% | 2.0 | 2 | 0.0% |
| 6 | 1 | -1 | 1 | 1 | -1 | 343.8 | 304.9 | -11.3% | 2.9 | 4 | 36.2% |
| 7 | -1 | -1 | -1 | 1 | -1 | 194.6 | 224.3 | 15.3% | 0.9 | 1 | 6.7% |
| 8 | 1 | -1 | -1 | 1 | 1 | 309.2 | 343.1 | 11.0% | 2.1 | 3 | 45.5% |
| 9 | -1 | -1 | 1 | 1 | 1 | 156.0 | 82.9 | -46.8% | 0.1 | 0 | -100.0% |
| 10 | 1 | 1 | -1 | -1 | 1 | 743.4 | 715.8 | -3.7% | 5.0 | 5 | 0.0% |
| 11 | 1 | 1 | -1 | 1 | 1 | 555.7 | 497.3 | -10.5% | 3.0 | 3 | 0.0% |
| 12 | 1 | -1 | 1 | -1 | 1 | 422.2 | 428.9 | 1.6% | 2.8 | 3 | 6.7% |
| 13 | -1 | 1 | 1 | 1 | -1 | 406.4 | 393.7 | -3.1% | 2.0 | 3 | 50.0% |
| 14 | 1 | 1 | 1 | -1 | -1 | 590.5 | 566.9 | -4.0% | 5.0 | 5 | 0.0% |
| 15 | 1 | -1 | -1 | -1 | -1 | 378.7 | 342.9 | -9.4% | 3.7 | 4 | 8.5% |
| 16 | -1 | 1 | -1 | -1 | -1 | 546.1 | 560.6 | 2.7% | 4.0 | 4 | 0.0% |
|  | -1 | -1 | -1 | -1 | 1 | 334.2 |  |  | 2.3 |  |  |
|  | -1 | -1 | -1 | 1 | 1 | 156.0 |  |  | 0.3 |  |  |
|  | -1 | -1 | 1 | -1 | 1 | 373.8 |  |  | 1.4 |  |  |
|  | -1 | 1 | 1 | 1 | 1 | 194.6 |  |  | 1.1 |  |  |
|  | -1 | 1 | -1 | 1 | -1 | 406.4 |  |  | 4.2 |  |  |
|  | -1 | 1 | -1 | -1 | -1 | 546.1 |  |  | 1.8 |  |  |
|  | -1 | 1 | 1 | -1 | 1 | 477.2 |  |  | 4.2 |  |  |
|  | -1 | 1 | 1 | 1 | 1 | 422.2 |  |  | 1.8 |  |  |
|  | 1 | -1 | -1 | 1 | 1 | 343.8 |  |  | 3.0 |  |  |
|  | 1 | -1 | -1 | -1 | -1 | 378.7 |  |  | 2.8 |  |  |
|  | 1 | -1 | 1 | 1 | 1 | 309.2 |  |  | 3.9 |  |  |
|  | 1 | 1 | 1 | -1 | -1 | 590.5 |  |  | 1.9 |  |  |
|  | 1 | 1 | -1 | -1 | 1 | 630.4 |  |  | 4.8 |  |  |
|  | 1 | 1 | -1 | 1 | 1 | 743.4 |  |  | 3.2 |  |  |
|  | 1 | 1 | 1 | -1 | 1 | 555.7 |  |  | 4.8 |  |  |
|  | 1 | 1 | 1 | 1 | -1 |  |  |  | 3.2 |  |  |

### 3.5    Locus of Failure

A cost-effective, in-house method for determining the locus of failure was one of the major goals set for this project.  The previous method involved sending inserts to The University of Dayton Research Institute (UDRI) where they performed X-ray Fluorescence (XRF).  This was a very effective method, but expensive and took time.  The goal was to move away from this in order to find a quicker and cheaper method.

The first method that was tried was using a phosphorescent sensor.  The two sensors that were implemented were: Dayglo D-034 Yellow and Phosphor Type 1260.   Both of these were added to UPSP-D and UPS-L (SPS-L already has a phosphorescent sensor in the adhesive formulation).  The results proved to be inconclusive.  The sensor did not seem to dissolve in the adhesive's solvents.  After pulling the AI, there was not enough dye on the rubber or steel to conclusively determine a locus of failure.

Another method that was explored was to mold AIs using the flat ends rather than the conical edge.  If adhesive failure occurred, this would yield a flat surface on both the rubber and the insert, which could be analyzed using ATR FT-IR.  A set of experiments using this method was used to determine the locus of failure.  The experiments were designed to look at the surfaces of the steel, and adhesive to determine if the failure was: RAF (adhesive only remains on the metal), MAF (adhesive only remains on the rubber), or cohesive adhesive failure (CAF) using ATR FT-IR.

The IR spectrum that was used to attempt to "see" the UPSP-D on the peroxide-cured rubber can be see in **Figure 62**.  This spectrum is an overlay of SPC sprayed with UPSP-D, UPSP-D film, and an SPC end of a part after pull.  There is not enough of a noticeable difference in the overlays to confidently assign a peak to the adhesive.
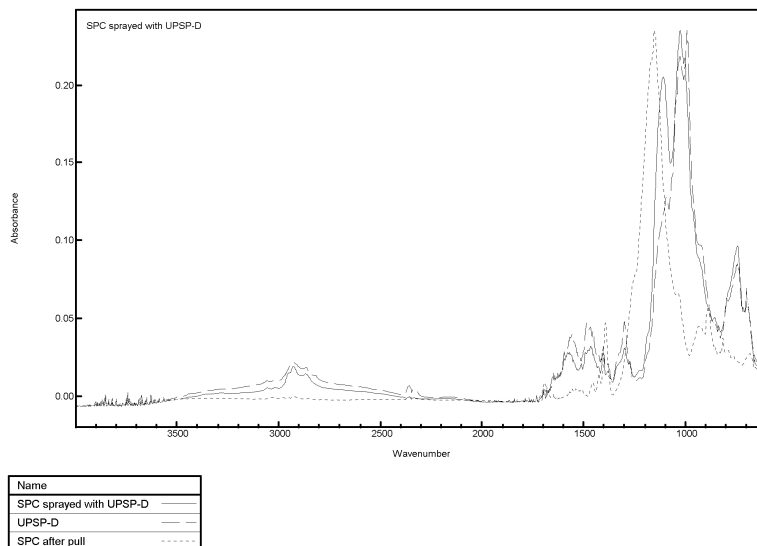


**Figure 62**: Tracking UPSP-D on SPC.

The same process was done with the steel insert to determine if the adhesive could be "seen" on it.  The spectrum in **Figure 63** is an overlay of the steel part of the sample after break, a clean steel insert, and the UPSP-D film.  There is a unique peak at 1125 cm$^{-1}$ on the sample after breaking it that might be indicative of the adhesive.
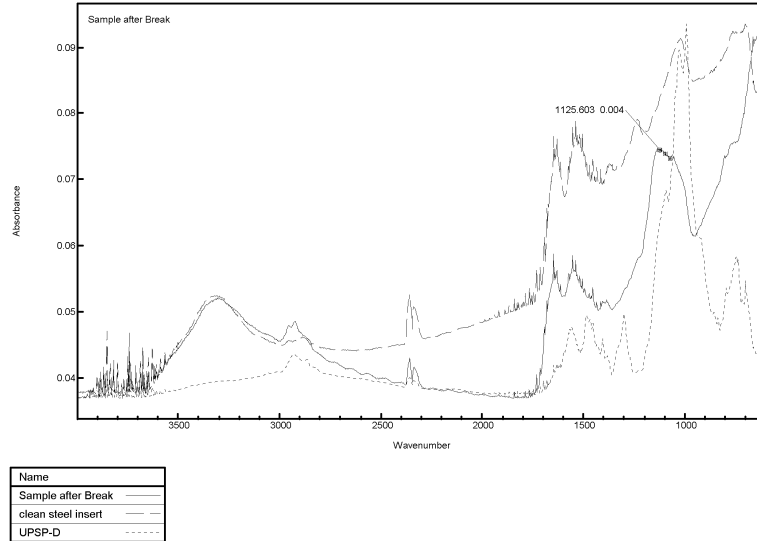
**Figure 63**: Tracking UPSP-D on steel insert.

At this point it is still inconclusive if, in fact, the peak at 1125 cm$^{-1}$ is evidence of the polymeric silane.  More tests such as x-ray photoelectron spectroscopy will need to be performed in order to confirm the presence of the polymeric silane.  If this proves to be the polymeric silane, it is believed that IR could be a step in the right direction to have an in-house method of determining locus of failure.

## 3.6    Window Dye Method

In an attempt to understand the tear mechanism a new method was developed to allow visualization of the tear process in real-time.  This method, called the "Window Dye Method", essentially involved molding half of the AI, leaving approximately half of the conical surface exposed.  An image of the profile can be seen in **Figure 19**.  After molding, these AIs were pulled on the extensometer and video was recorded.  The general tear mechanism was understood to be that the separation begins at the tip of the conical specimen and propagates from there.

One of the concerns was that, during the application process, the adhesive was flowing down the sides of the cone leaving a thinner layer at the tip, which would agree with the understood mechanism. To test this a few different application methods were utilized to determine if the tear mechanism could be manipulated. The inserts were dipped in adhesive, sprayed with adhesive then the tip of the insert was then dipped into the adhesive, held inverted during the entire process, and sprayed. Still shots from the video of the sprayed inserts can be seen in **Figure 64**. The still shots show the rubber beginning to separate from the metal (center) and no rubber retention, which was typical for all inserts.  All videos showed the tear mechanism being roughly the same no matter which method was chosen and very little rubber remained on the part.  This shows that the mechanism is likely not due to the flow of the adhesive.



**Figure 64:** SPC before pull (left), during pull (center), and after pull (right).

The window dye test can also be seen with the CC+TS system sprayed with UPSP-D, **Figure 65**.  The rubber seen left on the steel on the right still shot is essentially the 100% rubber failure seen with the combi-cured parts cured with ASTM D429 Method C.
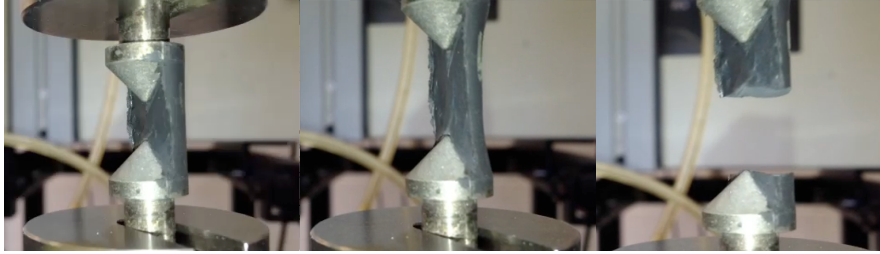
**Figure 65:** CC+TS before pull (left), during pull (center), and after pull (right).

## 4.        Conclusion

This study yielded many results involving adhering peroxide cured FKM to steel.  The most important being development of a formulation, "combi-cured with treated silica" that consistently yielded complete rubber failure when tested. Pretreatment methods were determined and optimized for cold-rolled steel and the use of two solvent rinses was found to be the optimal cleaning method.  Seven different adhesives were categorized based on their predicted curing.  The rubber formulation was then optimized to two of the three adhesive categories.  It was found that with the UPS-L adhesive the strongest bond was achieved using  Carbon Black, Treated Silica, Carnauba Wax, and Zinc Dimethacrylate while a combination of Carbon Black, Treated Silica, and Zinc Dimethacrylate was the best with the SPS-L adhesive. A method to determine the locus of failure using ATR FT-IR was started, but still needs to be optimized.

## 5.    Proposed Future Work

It is now well understood that cleanliness of the part is one of the more important factors to consider when adhering two surfaces.  It was found that solvent rinses were the best method to clean the part.  A realistic next step would be to determine which solvents would be best to clean the part.

Another direction to take the study would be to further optimize the rubber for the specific adhesives by looking at the other variables in the rubber formulation that were not considered.  Other results could be taken into consideration such as which ingredients in the formulation affect the cure time.  Do these ingredients also affect the adhesion?  Could the cure time be reduced?

Also, the exact mechanism is not well understood.  A logical next step would be determine if the adhesion in the "combi-cured" system curing truly behaves phenolic-like or if there is another mechanism that is being used.

# 6.    References

1. *http://www.kusumgar-nerlfi-growney.com/files/KNGGlobalAdhesivesIndustryBrochure2010.pdf* (accessed 05/26, 2013).

2. Mark, H. F. In *Fluorocarbon Elastomers;* Encyclopedia of Polymer Science and Technology; John C. Wiley and Sons: Hoboken, New Jersey, 2003; Vol. 2, pp 577-590.

3. Thomas, E. In In New Fluoroelastomer Developments for Aerospace Sealing Applications;2003.

4. Moore, A. L. *Fluoroelastomers Handbook: The Definitive User's Guide and Databook;* William Andrew Publishing: Norwich, NY, 2006; , pp 359.

5. Ameduri, B. From Vinylidene Fluoride (VDF) to the Applications of VDF-Containing Polymers and Copolymers: Recent Developments and Future Trends†. *Chemical Reviews* **2009**, 6632.

6. Améduri, B.; Boutevin, B.; Kostov, G. Fluoroelastomers: synthesis, properties and applications. *Progress in Polymer Science* **2001**, *26*, 105-187.

7. *http://www.webelements.com/fluorine/electronegativity.html* (accessed 04/28, 2013).

8. Kelly, J. Y. NOVEL FLUOROELASTOMERS COMPOSED of TETRAFLUOROETHYLENE and VINYLIDENE FLUORIDE OLIGOMERS SYNTHESIZED in CARBON DIOXIDE for USE in SOFT LITHOGRAPHY to ENABLE a PLATFORM for the FABRICATION of SHAPE- and SIZE-SPECIFIC, MONODISPERSE BIOMATERIALS, University of North Carolina, Chapel Hill, North Carolina, 2008.

9. Taguet, A.; Ameduri, B.; Boutevin, B. Crosslinking of Vinylidene Fluoride-Containing Fluoropolymers. *Adv Polym Scie* **2005**, *184*, 127-211.

10. Hiyama, T.; Yamamoto, H., Eds.; In *Organofluorine Compounds: Chemistry and Applications;* Springer: Heidelberg, New York, 1946; , pp 140.

## References (continued)

11. Sperati, C. A. In *Physical Constants of Fluoropolymers;* Brandrup, J., Immergut, E. H., Eds.; Polymer Handbook; John Wiley and Sons: 1989; pp V/35-V/43.

12. *http://inventors.about.com/library/inventors/blteflon.htm* (accessed 04/29, 2013).

13. Mark, H. F. In *Perfluorinated Polymers, Polytetrafluoroethylene;* Encyclopedia of Polymer Science and Technology; John Wiley and Sons: Hoboken, New Jersey, 2003; Vol. 3, pp 378-402.

14. *http://www.dynalabcorp.com/technical_info_ptfe.asp* (accessed 04/29, 2013).

15. *http://ezinearticles.com/?The-Many-Uses-of-Teflon-Or-PTFE&id=3412172* (accessed 04/30, 2013).

16. Mark, H. F. In *Vinylidene Fluoride Polymers;* Encyclopedia of Polymer Science and Technology; John C Wiley and Sons: Hoboken, New Jersey, 2003; Vol. 4, pp 510-533.

17. Vinogradov, A. M.; Holloway, F. Dynamic mechanical testing of the creep and relaxation properties of polyvinylidene fluoride. *Polym. Test.* **2000**, *19*, 131-142.

18. Duan, Y.; Yu, X.; Xue, Y.; Zeng, M.; Ji, S. Synthesis of Poly(vinylidene fluoride) with low content of head-to-head chain. *Poly. Comm.* **1983**, 161-167.

19. Esterly, D. M. Manufacturing of Poly(vinylidene fluoride) and Evaluation of its Mechanical Properties, Virginia Polytechnic Institute and State University, Blacksburg, Virginia, 2002.

20. Erhard, D. P.; Giesa, R.; Altstädt, V.; Schmidt, H. Synthesis and Structure-Property Relationships of Fluorinated Poly(ether imide)s as Electret Materials. *Macromolecular Chemistry and Physics* **2007**, *208*, 1522-1529.

21. Schildknecht, C. In *Vinylidene Chloride and Fluorovinyl Polymers;* Vinyl and Related Polymers; John C Wiley and Sons: New York, 1952; .

22. Hintzer, K.; Lohr, G. In *Melt Processable Tetrafluoroethylene-Perfluoropropylvinyl Ether Copolymers (PFA);* Scheirs, J., Ed.; Modern Fluoropolymers: High Performance Polymers for Diverse Applications; John Wiley & Sons: West Sussex, England, 1997; pp 223-237.

# References (continued)

23. Schmiegel, W. W. Die Angewandte Makromolekulare Chemie **1979**, 77, 39-65.

24. Schmiegel, W. W. *Kautschuk Gummi Kunstoffe* **1978**, *31*, 137.

25. Améduri, B.; Boutevin, B.; Kostov, G. Fluoroelastomers: synthesis, properties and applications. *Progress in Polymer Science* **2001**, *26*, 105-187.

26. Ameduri, B.; Boutevin, B. Copolymerization of fluorinated monomers: recent developments and future trends. *J. Fluorine Chem.* **2000**, *104*, 53-62.

27. Morton, M. In *Elastomer, Synthetic;* Kirk, Othmer, Eds.; Encyclopedia of Chemical Technology; John Wiley and Sons: Hoboken, NJ, 2004; Vol. 9, pp 550-567.

28. Science of Adhesion - What is Bonding? *http://www.adhesives.org/adhesives-sealants/science-of-adhesion* (accessed 05/06, 2013).

29. Gent, A. N.; Hamed, G. R. In *Adhesion;* Mark, H. F., Ed.; Encyclopedia of Polymer Science and Technology; John Wiley and Sons: Hoboken, NJ, 2003; Vol. 1, pp 218-256.

30. Why Does an Adhesive Bond? *http://www.adhesives.org/adhesives-sealants/science-of-adhesion/why-does-an-adhesive-bond* (accessed 05/06, 2013).

31. Marshall, S. J.; Bayne, S. C.; Baier, R.; Tomsia, A. P.; Marshall, G. W. A review of adhesion science. *Dental Materials* **2010**, *26*, e11-e16.

32. Yorkgitis, E. M. In *Adhesive Compounds;* Mark, H. F., Ed.; Encyclopedia of Polymer Science and Technology; Wiley-Interscience: Hoboken, NJ, 2003; Vol. 1, pp 256-290.

33. *http://www.specialchem4adhesives.com/resources/adhesionguide/index.aspx?id theory6* (accessed 05/14, 2013).

34. Possart, W. Experimental and theoretical description of the electrostatic component of adhesion at polymer/metal contacts. *Int J Adhes Adhes* **1988**, *8*, 77-83.

35. *http://www.chemicool.com/definition/coulombic_attraction.html* (accessed 05/14, 2013).

## References (continued)

36. Dunlap, D.; Parekhji, J.; Your, A. Interfacial Adhesion, 2002.

37. *http://www.specialchem4adhesives.com/resources/adhesionguide/index.aspx?id=theory4* (accessed 05/14, 2013).

38. *http://www.adhesives.org/docs/default-document-library/surfaceprep_adhesives-org.pdf* (accessed 05/14, 2013).

39. *http://science.jrank.org/pages/984/Bond-Energy.html* (accessed 05/15, 2013).

40. McMurry; Fay *Chemistry;* Pearson Education, INC: Upper Saddle River, NJ, 2012; .

41. *http://columbiaforestproducts.com/PureBond* (accessed 05/13, 2013).

42. Vachon et. al. California Patent 4,866,108, 1989.

43. Witucki, G. L. A Silane Primer: Chemistry and Applications of Alkoxy Silanes. *Coatings Technology* **1993**, *65*, 57.

44. Von Fraunhofer, J. A. Adhesion and Cohesion. *Intl. J. Dent.* **2012**, *2012*, 1-8- Article ID 951324.

45. *http://www.gifu-nct.ac.jp/elec/tokoro/fft/surface1.html* (accessed 05/07, 2013).

46. *http://www.uweb.engr.washington.edu/education/pdf/ASHsurfscontact%20angles05.pdf* (accessed 05/07, 2013).

47. *http://www.colloidaldispersions.com/shortcourse/private/Chicago07/Lecture%202%20 Wetting%20and%20adhesion.pdf* (accessed 05/07, 2013).

48. The ChemQuest Group Surface Treatment. *The Adhesive and Sealant Council, Inc* **2009**, 1-9.

49. Bebie, J.; Schoonen, M. A. A.; Fuhrmann, M.; Strongin, D. R. Surface Charge Development on Transition Metal Sulfides: An Electrokinetic Study. *Geochim. Cosmochim. Acta* **1998**, *62*, 633-642.

**References (continued)**

50. Plueddemann, E. P.; Pape, P. G. Surface Treatment of Industrial Minerals for Polymer Composites. *Colloque Les Mineraux Industrials Materiaux Des Annees* **1989**, *90*, 269.

51. Finzel, W. A.; Parr, L. M. Water-borne Silicone Alkyds and Acrylics. *Journal of Waterborne Coatings* **1979**, *2*.

52. Henning, S. K. Curing Elastomers with peroxides and coagents. *Rubber & Plastics News* **2010**, 12.

53. *http://www.columbianchemicals.com/rubber+carbon+black.aspx* (accessed 05/24, 2013).